C.P. No. 941

C.P. No. 941

MINISTRY OF TECHNOLOGY

AERONAUTICAL RESEARCH COUNCIL

CURRENT PAPERS

An experiment in Turbine Blade Profile Design

By

I. H. Johnston and Dianne Smart

LONDON: HER MAJESTY'S STATIONERY OFFICE

1967

Price 12s. 6d. net

U.D.C. No. 621.438-253.5:621.001.1

C.P. No. 941*
October 1965

An experiment in turbine blade profile design

- by -

I. H. Johnston and Diane Smart

SUMMARY

Part I of this Report describes a method for designing the blades of a highly loaded two-stage turbine on the basis of certain design parameters derived from an efficient turbine of lower loading. Part II presents the test performances measured with the original and new blades when tested in both single-stage and two-stage configurations. A full and detailed presentation of the experimental work is given to illustrate the problems in instrumentation and in interpretation of test measurements which were encountered.

The new blades give an improvement in the efficiency of the first stage, but the performance of the second stage remains unchanged and an analysis of blade section velocity distributions gives additional proof of the shortcomings of an essentially empirical design approach.

*Replaces N.G.T.E. R.274 - A.R.C. 27478

CONTENTS

CONTENTS (cont'd)

APPENDICES

ILLUSTRATIONS

ILLUSTRATIONS (cont'd)

1.0 Introduction

The aerodynamic design of a turbine stage to meet a specified duty comprises two fairly distinct phases.

Firstly it is necessary to select the vector diagram which will offer the optimum efficiency characteristic for the duty in question in the light of such restrictions on blade speed, blade temperature, turbine size and exhaust swirl as may be relevant.

Secondly the designer must prescribe a practicable blade geometry which will ensure that the above optimum performance is realised.

In the course of past turbine development and research, test data has emerged which has provided a basis for various broad correlations between turbine efficiency and the form of the vector diagram. Some of these (e.g., Reference 1) rest upon approximate correlations of profile and secondary losses for a wide range of turbine blades. Others are provided more directly by contour plots of efficiency (derived from test data) expressed as a function only of turbine stage loading $\left(\frac{2Kp\Delta T}{u^2}\right)$ and stage velocity coefficient (Va/u).

Whilst it is believed that such correlations can provide an adequate guide to the selection of an optimum vector diagram, experience suggests that the turbine efficiency for a particular vector diagram may still vary by a few points in efficiency dependent upon the detailed form of blade geometry (profile and pitching) selected by the designer. It is considered that such variations in efficiency are due, at least in part, to the inability of past design methods to provide the optimum blade geometry.

The reasons for this are partly historical. Until recent times, the blades in many gas turbines were designed using sections which were prescribed by three or more circular arcs following established steam turbine practice. As a result the blade forms did not follow any closely ordered sequence in terms of say, profile and camber line form, as has been the case in axial compressor design. A variety of simple design rules have been and still are used to set limits to physical features such as the blade back curvature and the passage width distribution along the inter-blade channel, but these have not always been successful in preventing the occasional disappointing turbine efficiency. This is not really surprising as such rules cannot properly define the complete blade profile and as a result the final shape can depend to a large extent upon the experience and judgement of the draughtsman concerned. Furthermore it is easy to appreciate that an optimum blade design is likely to require a more definite correlation between blade shape and aerodynamic loading.

In this situation the quite different approach of designing blades to provide specified surface pressure distributions is receiving an increasing amount of attention and is giving encouraging results. However the latter approach requires an extensive design effort which may well be beyond the resources of many organisations and there is therefore a continuing interest in the application of simpler methods which may be satisfactory for many applications.

In simple terms the problem is to identify those features of a blade design which play the dominant part in controlling blade losses and to then prescribe these features in the form of design parameters.

Part I of this Report describes a method used at N.G.T.E. some years ago to redesign the blading of a highly loaded turbine on the basis of certain design parameters derived from a more efficient turbine of lower loading.

Part II presents the test performance measured with the original 'datum' and new blades when tested in both single-stage and two-stage configurations.

Part I - The blade design

2.0 Background

The turbine which forms the subject of this investigation is a two-stage machine having an overall loading $\left(\frac{2Kp\Delta T}{u^2}\right)$ of 6.5 for the two stages. This value is not over-severe by current aircraft turbine design standards, but in this case the stage conditions are rendered more arduous due to the high flow per unit annulus area yielding Va/u values which are certainly above average. An additional difficulty is that the exit swirl from the second-stage is restricted so that the reaction at rotor root is zero.

When tested under cold flow conditions, the original blading for this turbine gave an expansion efficiency of approximately 87 per cent at the design point speed and pressure ratio, and, for the close tip clearance conditions which were operative, this efficiency was about 1 per cent less than that which might have been anticipated from the mean diameter vector diagram. It should be noted that the blading for this turbine was designed using pitch/chord ratio rules derived from cascade correlations and with blade profiles constructed from circular arcs.

During the development of the above turbine a second turbine was designed to provide the same power output with a larger diameter and reduced axial velocity. When tested at the same rotational speed and pressure ratio as the original datum turbine this larger unit gave an efficiency of 89.5 per cent i.e., an increase in efficiency of $2\frac{1}{2}$ per cent. Due to the larger diameter and consequently greater mean blade speed, the turbine loading $\left(\frac{2Kp\Delta T}{u^2}\right)$ was only 5.9 in comparison with the original 6.5, but when run at reduced speed to increase the loading to the latter value, the larger turbine still showed a superiority in efficiency of the order of 2 per cent.

The annulus forms of these two turbines are compared in Figure 1 which also lists the major aerodynamic stage design parameters.

In contrast to the circular arc blades of the original 'datum' design, the large 'reference' turbine used aerofoil blade sections constructed from prescribed thickness distributions set on parabolic (P40) camber lines, and the rotor blades were set at relatively closer pitch/chord ratios.

Taking the view that the superior performance of the larger turbine was unlikely to be due solely to the relatively modest change in stage vectors it was thought that a contributory factor towards its higher efficiency might be the design philosophy underlying its aerofoil blade design. Accordingly the blades for the smaller turbine were redesigned to incorporate the principle features of the aerofoil blading.

As this investigation was concerned primarily with securing an aerodynamic equivalence between the blades of the large turbine and those to be designed for the small turbine, no attempt was made to satisfy any specific blade stress requirements as it was considered that the first essential was to discover whether any improvement in aerodynamic performance could be obtained.

3.0 The design approach

The design details are discussed in the following sections.

3.1 The datum design

The design vector angles for the turbine blade rows are listed in Table I for root and tip reference diameters, and the leading dimensions of the datum blade design are shown in Table II.

TABLE I

Vector angles

		Stage 1			
		Stator		Rotor	
Reference diameter	(in.)	21.00	27.45	21.00	27.45
Gas inlet angle	(deg.)	0	0	47.30	18.00
Gas outlet angle	(deg.)	63.50	56.85	50.51	54.95
		Stage 2			
		Stator		Rotor	
Reference diameter	(in.)	19.925	28.525	19.925	28.525
Gas inlet angle	(deg.)	18.40	13.10	37.40	-1.10
Gas outlet angle	(deg.)	56.55	46.68	35.50	46.20

TABLE II

Details of datum blade design

		Stage 1			
		Stator		Rotor	
Reference diameter (in.)		21.00	27.45	21.00	27.45
Blade number		59		83	
Pitch	(s) in.	1.12	1.46	0.795	1.04
Chord	(c) in.	1.68	1.88	1.40	1.34
Axial chord	(c_a) in.	1.36	1.56	1.38	1.06
Throat	(o) in.	0.500	0.798	0.466	0.538
Maximum thickness	(t_m) in.	0.346	0.330	0.311	0.163
Trailing edge thickness	(t_e) in.	0.032	0.032	0.032	0.032

Average rotor tip clearance = 0.030 in.

		Stage 2			
		Stator		Rotor	
Reference diameter (in.)		19.925	28.525	19.925	28.525
Blade number		66		62	
Pitch	in.	0.948	1.358	1.010	1.445
Chord	in.	1.48	1.76	1.63	1.70
Axial chord	in.	1.27	1.63	1.61	1.35
Throat	in.	0.522	0.936	0.767	0.938
Maximum thickness	in.	0.286	0.315	0.216	0.097
Trailing edge thickness	in.	0.032	0.032	0.032	0.032

Average rotor tip clearance = 0.020 in.

As mentioned earlier these blades were constructed in the conventional manner using circular arcs. The profiles were required to have low curvature on the suction surface between the throat and trailing edge, and the channels between adjacent blades were made smoothly convergent up to the throat plane. The blade pitch/chord ratios were selected on the basis of general (primarily cascade) loss correlations.

3.2 The new design

The following parameters were selected to provide the means for translating the blade design of the large reference turbine into the requirements of the smaller turbine.

1. Blade loading
2. Profile shape
3. Thickness/pitch ratio

3.3 Blade loading

The Zweifel loading coefficient for a blade in cascade in terms of the pitch s, axial chord c_a and flow angles α_1 and α_2 is expressed as

$$\psi_t = 2s/c_a \, (\tan \alpha_1 + \tan \alpha_2) \cos^2 \alpha_2$$

This expresses the tangential lift force experienced by the blade section in incompressible flow as a proportion of the exit dynamic head. Thus for a given form of pressure distribution ψ_t provides a rough measure of the diffusion imposed upon the blade surface boundary layer.

The loading coefficients which were evaluated for the large reference turbine blades at the root and tip stations are compared with corresponding values for the datum design in the following table.

Blade loading coefficients

	Datum Turbine		Reference Turbine	
	Root	Tip	Root	Tip
1st Stator	0.655	0.855	0.580	0.81
1st Rotor	1.07	1.14	0.910	0.93
2nd Stator	0.88	0.97	0.85	1.23
2nd Rotor	1.30	1.03	1.05	0.92

Zweifel's original cascade work suggested that a loading coefficient of 0.8 was the optimum value but other test data derived from turbine test rigs has shown that the optimum mean loading coefficient for a given blade row may lie between 0.7 and 1.10.

A comparison of the loading factors showed that the major differences between the two designs concerned the rotor blade rows, the loading of the datum turbine being higher for both stages. The mean diameter values for the first stator rows were very similar and the average loading for the second stator row of the datum blades was slightly below that of the reference turbine. In the light of this comparison it was decided to limit the scope of the redesign to the rotor blades only. The method employed for each section was to combine the loading coefficient of the corresponding section of the reference turbine blade with the local vector angles of the datum turbine. In this way the appropriate values of pitch/axial chord for the root and tip sections of each rotor blade row were established.

3.4 Profile shape

The thickness distributions of the reference turbine are shown in Figure 2 and these were adopted for the new rotor blades. The parabolic (P40) camber line was also retained, the camber angles being modified to suit the datum vectors. Whereas the datum blading had been designed with approximately zero incidence at all sections the new blades were required to incorporate the same local incidences as the reference turbine, namely,

	Rotor 1		Rotor 2	
	Root	Tip	Root	Tip
Incidence (deg.)	+9.0	-4.0	+4.5	-6.0

3.5 Profile thickness

It is now well established that turbine efficiency is sensitive to the thickness of the blade trailing edges, and various analyses of this effect indicate that the ratio trailing edge thickness/blade pitch is the significant parameter against which loss in efficiency may be correlated. For this reason the (t_m/s) values of the reference blade sections were used to define the thickness of the new blades in preference to the more conventional maximum thickness/chord ratio. However it was found that the resulting blade geometry at the root of the second-stage rotor gave a channel throat upstream of the trailing edge. This was alleviated by reducing the originally calculated value of (t_m/c) from 13.5 to 11.2 per cent.

3.6 Design summary

The above paragraphs indicate the main considerations which entered into the design of the new blades, particulars of which are listed in Table III.

TABLE III

Details of new rotor blade design

		Stage 1 rotor		Stage 2 rotor	
Reference diameter	in.	21.00	27.45	19.925	28.525
Blade number		101		73	
Pitch	in.	0.654	0.854	0.858	1.226
Chord	in.	1.44	1.26	1.64	1.67
Axial chord	in.	1.34	1.06	1.60	1.34
Throat	in.	0.397	0.439	0.660	0.764
Maximum thickness	in.	0.227	0.1016	0.183	0.066
Trailing edge thickness	in.	0.027	0.024	0.022	0.016
Average rotor tip clearance	in.		0.038		0.014

The blade profiles at each station were finalised by an iterative graphical procedure whereby the stagger angle was varied with the aim of making the total throat areas of the new blades equal to those of the datum blades. In the event this aim was not exactly realised, the throat area of the new first-stage blades being approximately 1 per cent higher and that for the new second stage blades 1 per cent lower than in the datum blade design. However these variations should have little effect on stage efficiency, the differences in relative outlet angle being less than half a degree, and we can therefore relate changes in efficiency to the effect of profile shape.

For record purposes the ordinates which define the root and tip sections of the datum and new blade designs are recorded in Appendix II.

Part II - Experimental investigation

4.0 Background

The experimental evidence regarding turbine efficiencies which is referred to in Part I and which triggered off this investigation was acquired in the course of engine development testing. This early work was confined to a very restricted range of turbine operating conditions and accordingly it was decided that in addition to testing the new blade design the performance of the original (datum) blading should be examined in some detail.

The test programme comprised four test series in which first the original blades and then the new blades were tested in both two-stage and single-stage configurations. A brief description of this test work is given, and the test results are presented and discussed in the following sections.

5.0 The test facility

The general layout of turbine and the associated ducting is illustrated in Figure 3. Air at about 130°C was supplied from plant compressors and passed via an I.S.A. flow nozzle to a plenum chamber (collector box) and thence to the turbine. At exit from the turbine blades the air passed through a parallel annulus and then exhausted to atmosphere via the exhaust cone, jet pipe, and silencer ducting. The turbine rig was originally designed for both cold and hot running and the complete unit consisted of an engine combustion system followed by the turbine. For the work under review there was no requirement for hot running so the burners and flame tubes were removed from the combustion space and replaced by a sheet metal bell mouth entry section and a parallel annulus upstream of the nozzle blades (see Figure 4). In this modified arrangement air from the entry volute suffered an abrupt expansion into the combustion space and it was considered that the subsequent acceleration through the annular bell mouth would be sufficient to give uniform conditions at the turbine entry.

Figure 4 also shows the distributions of total pressure and axial velocity measured at the turbine inlet section at three circumferential stations and although total pressure is reasonably uniform it is evident that there is some variation in axial velocity in both the radial and circumferential directions. It was decided to accept these conditions for the present test work with the reservation that the sensitivity of turbine performance to variations in inlet velocity distributions should be investigated at a later date.

The power from the turbine was absorbed by a Heenan and Froude high speed water brake with a maximum capacity of 10,000 h.p. at 10,000 rev/min.

6.0 Instrumentation

6.1 Air mass flow

Air flow measurement was by a 20 in. diameter I.S.A. nozzle situated in the 34 in. inlet duct (see Figure 1). Prior to the turbine tests a check calibration of this measuring system was made by replacing the turbine rig with a long length of ducting in which an orifice plate was installed to the requirements of BS.1042. For the conditions of the test the nominal tolerances for both nozzle and orifice were assessed as ±1 per cent. However it was encouraging to find that the agreement between these two dissimilar meters was very much closer, the maximum difference being 0.1 per cent. On this evidence the nominal constant for the I.S.A. nozzle was accepted for the evaluation of mass flow during the test series.

6.2 Turbine air pressures

The positions for the measurement of total and static air pressures in and around the two-stage turbine are illustrated in Figure 5.

Turbine entry (plane CC). Inlet total pressure (P_1) was measured using three, five-point Kiel rakes. In addition eight static pressure tappings (p_{1o} and p_{1i}) were provided at both the outer and inner annulus walls.

1st stator exit (plane DD). Static pressure tappings were provided into the space between stator and rotor below the annulus wall (p_{2i}) and on the outer wall (p_{2o}). In locating the tappings on the outer wall a range of circumferential positions relative to the stator trailing edges was covered.

1st rotor exit (plane EE). Eight pressure tappings were provided in the outer annulus wall (p_{3o}) and three in the space between the rotor disc and the second stator diagram (p_{3i}). The latter tappings were connected via lengths of hypodermic tubing which were set into channels in the leading edge of three second-stage stator blades.

2nd stator exit (plane FF). Four static tappings in the outer annulus wall (p_{4o}).

Turbine exit (plane GG). An array of wall static tappings in both outer and inner walls (p_{5o} and p_{5i}) were located approximately 2 in. downstream of the rotor blades in the parallel exit measuring section.

Two forms of total pressure (P_5) measurement were adopted in this section.

(a) Three Kiel rakes each with five points set at centres of equal area.

(b) Three cylindrical instruments carrying pitot and yaw tappings at five radial stations. These instruments were remotely controlled and required to be yawed for each individual pressure reading.

6.3 Turbine air temperatures

Air temperature at turbine inlet (T_1) was measured using three thermocouples in stagnation shields set in the entry volute, in which the temperature was uniform. The temperature at turbine exit was measured at two planes JJ in the exit measuring section by 23 instruments set at varying radial positions.

6.4 Single-stage instrumentation

For tests of the single-stage configurations a modified outlet measuring section was fabricated which could be inserted into the space formerly occupied by the second stage blading. This arrangement is illustrated in Figure 6 and the measuring positions are indicated. The wall

static pressure tappings in the plane GG were used in the assessment of turbine performance. Other wall static tappings were located at two downstream stations, F_1 and F_2, but these were not used in the present investigations.

Total pressure was measured using three five-point Kiel rakes and for some tests the cylindrical instruments from the two-stage tests were also adapted. These were of limited use as the radial positions of their sampling points no longer conformed to equal area stations for the reduced annulus height.

6.5 Traversing

At an early stage in the test work it became apparent that the standard of yaw angle measurement obtainable using the cylindrical instruments was of indifferent accuracy and accordingly a remote controlled traverse gear was installed with an arrowhead pitot yawmeter. This was mounted in place of one of the cylindrical instruments and provided detailed measurements of pressure and flow angle.

7.0 Test results

7.1 Series 1

The test performance for the datum blading was measured at four non-dimensional speeds, and characteristics of efficiency, flow and outlet swirl are plotted in Figures 7, 8 and 9.

The efficiency values of Figure 7 were derived in the following way:

$$\eta = \frac{\Delta T}{\Delta T'}$$

where ΔT is the temperature drop equivalent of the work output, calculated from measurements of brake torque, rev/min and air mass flow; and $\Delta T'$ is the isentropic temperature drop corresponding to the measured inlet temperature and total head pressure ratio. The pressure ratio was based on the measured inlet total pressure and on an outlet total pressure calculated from average swirl angle, static pressure and mass flow.

The reason for preferring this 'continuity' pressure to a directly measured values is evident from consideration of Figure 10 where efficiency characteristics calculated using the measured exit total pressures are shown.

It will be observed that for the design speed curve the efficiency values calculated using arithmetic mean values for the exit total pressure have been subdivided in respect of the two types of instrument used for measurement. Superficially, it would appear that the cylindrical rakes record higher pressures than do the Kiel rakes, and also the rising form of the $\left(\frac{N}{\sqrt{T_1}} = 263 \right)$ efficiency characteristic at pressure ratios above 2.8 appears suspicious.

The individual outlet total pressure measurements for two test points are shown in Figure 11 in the form $\frac{\text{local dynamic head}}{\text{mean dynamic head}}$ and it is clear that at any radius there is considerable scatter in total pressure. It is also evident that a relatively small change in turbine pressure ratio causes a considerable change in the exit pressure distribution. This change in relative pressure at a fixed circumferential position was further examined by comparing the mid-annulus measurements of a single instrument with the calculated average values for a range of turbine operating conditions. Figure 12a shows the cyclic variation in local pressure and it is evident that the amplitude of pressure variation is significant when expressed as a change in turbine efficiency. In an attempt to identify the source of this pressure variation a simple mean diameter analysis was carried out to assess the circumferential movement at the measuring plane of a wake from a second-stage stator blade. The result of this calculation is shown in Figure 12b as a plot of circumferential movement against turbine pressure ratio. The minimum pressures in Figure 12a occur at turbine pressure ratios of 2.02 and 2.8 and this corresponds to a calculated circumferential movement of 1.10 inches. This agrees very closely with the 1.153 in. pitch of the second-stage stators at mean diameter and gives convincing support to the view that the non-uniformity of total pressure measured at turbine exit is due to the presence of stator blade wakes in the exit flow.

The circumferential positions for the six total pressure rakes had been selected to provide some variation with respect to the second-stage stator blades. Thus a very rudimentary pitch-wise traverse was available with respect to the fixed blades as shown in Figure 13a. This shows that two of the circumferential positions were duplicated and it was thought that a weighting of the pressure measurements to account for this should be examined. Mean exit pressures were accordingly recalulated as shown in Figure 13b but the effect on the efficiency characteristic was marginal.

It was concluded that any average total pressure deduced from the direct measurements would be open to suspicion and, although total pressures were recorded for this and the following test series, interest was concentrated on those efficiency values which were derived by using calculated exit total pressure.

During the course of the testing, the torque weighing system was frequently checked and proved to be satisfactory. Figure 13c provides a comparison between the efficiency characteristic derived from the brake readings and that deduced from the measured temperature drop. Up to a pressure ratio of 2.9 the comparison is very satisfactory with the brake values approximately $\frac{1}{2}$ per cent lower. As the pressure ratio is increased above 2.9 the gas velocity in the exit section increases rapidly and it is probable that the discrepancy between thermocouple and brake efficiencies is due to imperfect temperature recovery by the exit thermocouples.

After the characteristics shown in Figures 7 to 10 for the datum blading were obtained, the test work was abruptly terminated by the fatigue failure of the second-stage rotor blades which were made of aluminium.

The turbine was then stripped and rebuilt as a single-stage unit for the tests of Series 2.

7.2 Series 2

The test characteristics for the single-stage assembly of the original 'datum' blading are shown in Figures 14 to 17 for four speeds including the design value $\left(\frac{N}{\sqrt{T}} = 263\right)$ and a 10 per cent overspeed. The outlet measuring section was smaller than for the Series 1 tests and three new Kiel rakes were fitted to provide equal area samples. In addition, for the early tests of Series 2 the cylindrical probes were also included. Although each could provide only four sampling points due to the reduced height of the annulus they did improve the circumferential coverage and provided some swirl measurement.

The results obtained with this instrumentation are shown in Figure 17 and were even more scattered than for Series 1. Naturally, the effects of variation in outlet pressure upon efficiency were greater due to the exit dynamic head now representing a much greater proportion of the total pressure drop over the turbine. In addition the total pressure observed with the cylindrical probes appeared to exceed that from the Kiel instruments at all conditions. An attempt was made to examine this phenomenon by transposing two instruments. This seemed to confirm that the cylindrical probe gave a higher reading than the Kiel rake, but as the radial positions of measurement were different for the two types of instrument and in view of the difficulty of obtaining precisely repeatable flow conditions in the rig this check was not conclusive.

These difficulties regarding the measurement of outlet total pressure encouraged reliance, as in Series 1, on a continuity assessment of pressure. However, at design point conditions, the exit swirl from the single-stage unit was 25° to 30° and so the calculated pressure, and hence efficiency, was critically dependent on the value of swirl angle. Instead of the cylindrical probes, an accurate traversing pitot yawmeter was used. By using the locations formerly occupied by the cylindrical probes it was possible to demonstrate a satisfactory circumferential distribution of swirl angle ($\pm 1^{\circ}$) at any radius. On this evidence, for this and subsequent test work, the swirl measurements obtained from radial traverses at a single circumferential station were used for the evaluation of exit total pressure and hence efficiency.

The plane of measurement of outlet total pressure was only half a blade chord downstream of the rotor blade, so to assess the importance of axial spacing a check test was made with the total pressure instrumentation moved approximately four blade chords further downstream of the rotor blades. The effect of this was to reduce the difference in the total pressures recorded by the Kiel and cylindrical probes, but the level of the resultant efficiency was about 1 to 2 per cent lower than that based on the Kiel measurements at the upstream instrumentation plane.

One conclusion from these investigations concerning outlet pressure measurement was that the mean value based on Kiel probes close to the rotor was in tolerable agreement with the pressure assessed by continuity. However the variations which were obtainable by changes in either the number, type, or position of the instruments were such as to render any

direct measurement open to suspicion. For this reason, although the outlet total pressures were still measured in the further work of Series 3 and 4 and are recorded in the tables of results, the critical assessments of stage efficiency were based on exit total pressures calculated by continuity.

7.3 Series 3

Following the single-stage tests of Series 2 the turbine was stripped and rebuilt with the new rotor blades as a two-stage unit. The test arrangements were similar to those of Series 1 except that the cylindrical probes at turbine exit were dispensed with and an additional traverse point was provided in the leading edge plane of the second-stage stators.

Test work was restricted to two speeds and the performance characteristics are shown in Figures 18 to 20.

At the design speed and a pressure ratio of approximately 2.9, inter-stage traverses for total pressure, static pressure, flow angle and total temperature were carried out. The second-stage stators were inclined at an angle of about 10° from the radial and as the traverse probe was located between the blades it was necessary for the probe also to be inclined from the radial direction.

A five-hole instrument was used, the head of which carried a central pitot hole with two pairs of yaw holes. This instrument was calibrated in a tunnel by balancing the yaw pressures in the plane normal to the stem of the instrument, and correlating the pressure difference measured at the other yaw holes with the angle between the flow and the instrument.

By using this instrument it was possible to measure air flow angles in the tangential and radial directions.

7.4 Series 4

For the final tests of this sequence the second-stage was removed to permit a test of the first-stage blades as in Series 2. Performance characteristics are shown in Figures 21 to 23 for the three speeds which were examined.

7.5 Presentation of results

In addition to the characteristic performance curves, representative test information is recorded in Appendix III. Where values for inter-blade row static pressures are quoted, these are the arithmetic mean values for each location. Figure 24 illustrates the circumferential distributions of the individual readings for the 'design point' of each series. It may be observed that the interstage outer wall statics show marked circumferential variation. This improves for the single-stage tests so it is probable that the variation in pressure was due to the presence of the second-stage stators.

8.0 Discussion

8.1 Comparison of test efficiencies

The test performances for the datum and new blading are compared in Figure 25 where the efficiencies for both two-stage and single-stage assemblies are plotted against the loading parameter $\left(\frac{2K_p\Delta T}{u^2}\right)$. At the single-stage design conditions $\left(\frac{2K_p\Delta T}{u^2} = 3.8\right)$, the change in rotor blade design gives a rise in efficiency from 86.5 per cent to 89 per cent. This improvement, 2.5 per cent, is not maintained for the two-stage assemblies where the change in efficiency is from 86.5 to 88 per cent. Indeed, the above figures suggest that the change in blade design of the second-stage has no effect on the efficiency of that stage.

To examine these effects in greater detail the flow conditions were analysed on the basis of stator blade loss coefficients assessed by the methods of Reference 1, and the resultant rotor blade loss coefficients are shown in the following table.

	Pressure Loss Coefficients		
	Datum	New	Estimate
1st stage stator	0.06	0.06	0.06
rotor	0.22	0.16	0.20
2nd stage stator	0.13	0.13	0.13
rotor	0.12	0.12	0.10

It will be observed that only one estimate of loss is quoted for each blade row. This is because the method of assessment is insensitive to the changes in pitch/chord ratio of the present investigation.

The figures for the first-stage rotor indicate that the loss of the datum blade is 10 per cent higher than the estimated value, this being equivalent to approximately 0.8 per cent in efficiency. The improvement in stage efficiency of 2.5 per cent obtained with the new blades is seen to be equivalent to a reduction in rotor loss coefficient of 27 per cent.

As mentioned previously, the second-stage efficiency deduced from the two-stage results is not affected by the change in blade design and the blade loss coefficients therefore remain the same.

8.2 Comparison of flow characteristics

Comparison of the flow characteristics presented in Figures 8, 15, 19 and 22 shows that for both datum and new blade designs, the choking flows for the two-stage turbines are less than those for the single-stage turbines. By analysis of axial pressure distributions through the blade rows it can be shown that the choking plane for the two-stage turbines is located in the low pressure stator blades and the reduction in flow relative to the single-stages is therefore logical. It is more difficult to understand the increase in choking flow of approximately 0.5 per cent between the new and datum two-stage assemblies when clearly they both incorporate the same choking blade row. The only explanation would seem to be that the improvement in first-stage efficiency obtained with the new first-stage rotor blades must provide more uniform flow conditions to the low pressure stator blades, thereby improving the flow coefficient of the stator blade row.

Comparison of the single-stage flow characteristics indicates that although the flows for datum and new blades are similar at low stage pressure ratio, the choking flow with the new blades exceeds that for the datum blades by approximately 1.0 per cent. This is accountable to the difference in rotor blade row throat area reported in Section 3.6 as in these single-stage turbines the choking plane is located in the rotor blade row and not, as is more usual, in the stator row.

8.3 Traverse data

During the testing of the single-stage assemblies, radial traverse measurements of pressure and flow angle were made at turbine exit and typical distributions of axial velocity, total pressure, and swirl angle for both the datum and new blades are shown in Figure 26. At the time of these tests it was not possible to provide means for circumferential movement of the traverse instrument and the values in Figure 26 were obtained by simple radial traverses.

Using these traverse measurements the flow angles relative to the rotor blades were calculated and the radial distributions of relative angle are compared in Figure 26 with the original design angles and with angles estimated by the method of Reference 1. It is evident that the latter estimates give reasonable approximations to the mean flow angles. The original design angles were linked with the assumptions of free vortex flow and uniform axial velocity, but it is evident that the axial velocity is far from uniform. To assess the significance of rotor exit angle a radial equilibrium assessment of the flow conditions within the blading was made using the estimated values of rotor outlet angle for the new blades. The resultant axial velocity distribution is shown in Figure 26 and although it differs considerably from the measured value it gives a partial explanation for the general slope of the measured axial velocity distribution.

The results of traverses at many other test conditions are illustrated in the bottom diagrams in Figure 26. These show the mean relative outlet angles calculated from traverse measurements plotted against the relative outlet Mach number. The straight lines are interpolations between values estimated for Mach numbers 0.5 and 1.0 following the methods of Reference 1. The test figures confirm the estimated trend of increasing

angle with Mach number and generally provide satisfactory confirmation of the methods currently used for the assessment of the relative outlet flow angle from a turbine blade row.

8.4 Interstage measurements

As mentioned in Section 7.3 an attempt was made to measure interstage conditions in the course of the tests on the two-stage build of the new blading. Traverses for pressure, angle and temperature were made using an arrow head pitot yaw probe and a shielded thermocouple which were each traversed at a position midway between the leading edges of adjacent second-stage rotor blades. The five-hole pitot yaw probe was calibrated to give total pressure, static pressure and radial flow angle, in addition to the circumferential flow angle, and the traverse results are shown in Figure 27. The upper row of results were obtained with the two-stage build, and the lower row are for the single-stage build with the traverse gear mounted in the 'interstage' position.

Due to the proximity of the traverse probe to the second row stator blades and the relatively close pitch of the latter it was inevitable that some interference effect would be encountered. This is illustrated in the plot of static pressure which indicates a significant difference in level between the measurements with the probe near the walls of the annulus and the wall static values. This may be contrasted with the tolerable agreement between these forms of measurement obtained with the single-stage test. The low static pressures of the first traverse are no doubt accountable to the blockage effect of the traverse instrument in relation to the stator blades. It was found that to obtain reasonable agreement between mean axial velocity (based on mass flow and annulus area) and velocity calculated from traverse pressures it was necessary to correct the traverse values of static pressure up to the level indicated by the wall measurements. Despite this, it is of interest to note that the radial variation of static pressure indicated by the traverse is in agreement with the difference between the inner and outer wall measurements. To this extent the traverse result corroborates the 'inverse' pressure gradient* indicated by the wall statics, a phenomenon which has been reported for other two-stage turbines. In addition to the static pressure 'inversion' the interstage traverses reveal radial variations in total pressure, total temperature and radial flow angle which are greater than those observed in the single-stage test. It will be observed that the stage pressure ratio for the single-stage traverse is significantly greater than that for the two-stage test. This failure to reproduce the exact stage loading was attributable in part to the setting-up condition which was aimed at, namely a similar value of $\frac{\bar{p}_3}{p_1}$ where $\bar{p}_3$ was taken as the mean of the wall static pressures. Due to the difference in form of the radial distributions of static pressure, the true mean expansion ratio for the single-stage test would have been high even if the nominal setting-up conditions had been satisfied exactly.

*With swirling flow in an annulus it is customary to expect a radial gradient of static pressure such that p_{stat} increases with radius. An 'inverse' gradient would seem to indicate strong outward components of radial flow.

Fortunately the single-stage traverse data at this 'interstage' position was found to be in tolerable agreement with other traverses taken in the normal instrumentation plane for single-stage testing and these results, which cover a range of stage operating conditions, indicated that the radial variations of flow conditions did not change significantly for a moderate range of stage pressure ratios. It is therefore not unreasonable to compare the radial distributions shown in Figure 27 for the two-stage and single-stage builds.

Axial velocity profiles and radial distributions of stage temperature drop were computed and are shown in Figure 28. If end effects are ignored it is seen that the axial velocity for the two-stage build tends to reduce from tip to root, i.e., in reverse direction to that of the single-stage. This change in distribution is confirmed by the curves for stage temperature drop, the two-stage build showing a significant reduction in temperature drop from tip to root in comparison with the single-stage version.

It is clear that detailed flow measurements of this type are subject to many qualifications due to the instrumentation difficulties which abound. Nevertheless the results of the present investigation appear to provide conclusive evidence that the flow conditions within the first turbine stage are influenced by the presence of a closely following blade row.

9.0 Blade surface velocities

In the general introduction to this paper mention was made of an increasing interest in the relation between blade profile design and surface velocity distributions. The simplest assessment of velocity distribution is provided by the stream filament analysis and using this approach the root and tip sections of the datum and new rotor blades were examined. The surface velocity distributions for two-dimensional compressible flow were calculated and significant portions of the suction surface velocity distributions are reproduced in Figure 29. As the analysis is basically a channel method the values calculated downstream of the throat are inevitably open to question as they depend upon an assumed form for the trailing edge streamline. Accordingly these portions of the distributions are shown as dotted lines, and must be taken with reserve.

In order to assess the significance of surface velocity distributions it is convenient to make use of a simple criterion for velocity gradient. Other work has shown that for a simple triangular velocity distribution a wholly turbulent suction surface boundary layer should be free from separation provided the velocity gradient is less than 0.5. That is to say the leading edge velocity of such a triangular distribution must be not more than 50 per cent greater than the exit velocity.

Examination of Figure 29 shows that the datum design for the first stage root section has a local velocity gradient which far exceeds this criterion and it is probable that the increase in the first-stage efficiency obtained with the new blades is due to the suppression of boundary layer separation by virtue of the marked improvement in velocity distribution of the root section.

In the second-stage blades, the calculations for the tip sections indicate a steeper velocity gradient for the new blades, but this occurs downstream of the blade throat where the distribution of velocity depends on the form assumed for the trailing edge streamline. If consideration is restricted to the more accurately defined velocities within the blade channel (upstream of the throat) the distributions do not suggest any major difference in boundary layer behaviour and to this extent are in line with the efficiency measurements for the second-stage blading.

It may be noted that the overall loss coefficient is apparently unchanged between datum and new designs in spite of the fact that the blade surface area has been increased by 18 per cent in the new design. Lower loading would seem to have resulted in a reduction in boundary layer growth (or separation) sufficient to compensate for the greater surface area. It seems possible that the optimum loading factor may lie somewhere between the values related to the two designs. It would also appear that there is scope for further modification of both the tip profiles, such as to increase the loading over the leading section of the blades, and thereby to enhance the efficiency of the tip regions of both stages.

10.0 Conclusions

1. These tests have yielded positive confirmation of a number of errors and problems of instrumentation commonly pertaining to turbine testing.

   (a) The direct measurement of total pressure at exit from a turbine is liable to error from a variety of sources.

   (b) At a measuring station at least one blade chord downstream of the second-stage rotor there is evidence of significant maldistribution due to the presence of unmixed stator wakes in the exit flow.

   (c) It is suspected that cylindrical pitot instruments are particularly unsuitable for pressure measurement downstream of a moving blade row.

   (d) There is some evidence that the exit swirl from a turbine is uniform circumferentially, but further test work with suitable instrumentation is required to substantiate this claim.

   (e) Inter-row wall static pressures are sensitive to their circumferential position with respect to fixed blades.

2. The methods in use at N.G.T.E. for the estimation of flow outlet angles from turbine blades are well substantiated by the agreement between estimated angles and those deduced from the test data.

3. There is some evidence that the radial flow pattern within a turbine stage can be significantly affected by the presence of a following stage.

4. The efficiency of one turbine stage has been significantly improved by a change from circular arc blading to aerofoil blading of lower pitch/chord ratio. The insensitivity of the second-stage efficiency to a similar design change emphasises the hit and miss nature of such empirical design methods.

5. A $2\frac{1}{2}$ per cent increase in first-stage efficiency is attributed to a reduction in suction surface diffusion at the rotor blade root. Although this improvement was obtained using a blade of a particular aerofoil section at a loading coefficient of 0.91 it is probable that a variety of blade shape/loading combinations might have accomplished a comparable improvement in local velocity distribution and a similar increase in stage efficiency.

6. It is considered that when empirical methods are used for the design of blade sections the surface velocity distributions should be examined to ascertain the diffusion gradients involved. More data is required, however, to identify critical design limits to these distributions and gradients with better confidence; although the present tests have provided at least an example of designs lying on the right and wrong side of such a limit.

11.0 Acknowledgements

The authors wish to acknowledge the valuable assistance provided by Mr. C. K. Roberts who was responsible for the installation and mechanical operation of the test rig; by Miss J. Marshall who acted as test observer and carried out much of the computation required during the investigation; and by Mr. D. J. L. Smith who was responsible for the blade surface velocity analysis.

REFERENCE

No.	Author(s)	Title, etc.
1	D. G. Ainley G. C. R. Mathieson	A method of performance estimation for axial flow turbines. A.R.C. R.&M. No. 2974, December 1951

APPENDIX I

Notation

K_p	Specific heat of air at constant pressure
L	Brake load (lb) $\quad (HP = L \times \frac{N}{2000})$
M	Air mass flow (lb/s)
N	Rotational speed (rev/min)
P_1	Turbine inlet total pressure (in.Hg)
$P_{5\,calc}$	Turbine exit total pressure deduced by continuity
P_{5meas}	Turbine exit total pressure measured directly
p_{1o}, p_{1i}	Wall static pressures at turbine entry
p_{2o}, p_{2i}	Wall static pressures after first row stator blades
p_{3o}, p_{3i}	Wall static pressures after first-stage rotor blades
p_{4o}	Wall static pressure after second-stage stator blades (outer wall only)
p_{5o}, p_{5i}	Wall static pressures in exit measuring plane
T_1	Turbine inlet temperature (^oK)
T_5	Turbine exit temperature (^oK)
ΔT	Turbine temperature drop (^oC)
V_a	Axial velocity (ft/s)
u	Mean blade speed (ft/s)
α_5	Exit swirl angle (degrees)
β	Radial flow angle (degrees)
η	Efficiency

APPENDIX II

Blade profile ordinates

x = chordwise position from leading edge

y_p = ordinate from chord line to concave surface

y_s = ordinate from chord line to convex surface

Stator 1

Root (10.50 in. radius)
LER = 0.095 in. TER = 0.016 in.
Stagger angle 36 deg.

x	y_p	y_s
0	0.095	0.095
0.05	0.011	0.1875
0.10	0	0.242
0.20	0.0285	0.323
0.30	0.0578	0.382
0.40	0.082	0.422
0.50	0.1015	0.447
0.60	0.116	0.4585
0.70	0.1285	0.457
0.80	0.132	0.4415
0.90	0.1338	0.413
1.00	0.131	0.372
1.10	0.123	0.3245
1.20	0.112	0.277
1.30	0.097	0.227
1.40	0.076	0.176
1.50	0.050	0.1238
1.60	0.020	0.0698
1.68	0.0175	0.0175

Tip (13.725 in. radius)
LER = 0.095 in. TER = 0.016 in.
Stagger angle 34.1 deg.

x	y_p	y_s
0	0.097	0.097
0.05	0.012	0.190
0.10	0	0.2425
0.20	0.031	0.325
0.30	0.065	0.3838
0.40	0.094	0.423
0.50	0.118	0.448
0.60	0.137	0.460
0.70	0.152	0.4585
0.80	0.162	0.443
0.90	0.168	0.417
1.00	0.1695	0.385
1.10	0.167	0.3515
1.20	0.1595	0.316
1.30	0.148	0.278
1.40	0.132	0.240
1.50	0.112	0.1995
1.60	0.087	0.157
1.70	0.057	0.1125
1.80	0.0218	0.065
1.878	0.018	0.018

APPENDIX II (cont'd)

Rotor 1 (datum design)

Root (10.33 in. radius) LER = 0.0375 in. TER = 0.016 in. Stagger angle 10.10 deg.			Tip (13.862 in. radius) LER = 0.0335 in. TER = 0.016 in. Stagger angle 37.5 deg.		
x	y_p	y_s	x	y_p	y_s
0	0.037	0.037	0	0.0336	0.0336
0.05	0.002	0.1868	0.05	0.0042	0.1292
0.1	0.036	0.2685	0.1	0.0433	0.187
0.2	0.0975	0.378	0.2	0.1007	0.2617
0.3	0.145	0.447	0.3	0.1384	0.3019
0.4	0.1805	0.492	0.4	0.1585	0.3184
0.5	0.206	0.517	0.5	0.1636	0.3112
0.6	0.2195	0.5235	0.6	0.1527	0.2844
0.7	0.225	0.5145	0.7	0.1342	0.2525
0.8	0.220	0.4878	0.8	0.1149	0.2211
0.9	0.206	0.4415	0.9	0.0956	0.1879
1.0	0.182	0.374	1.0	0.0755	0.1543
1.1	0.147	0.297	1.1	0.0534	0.1191
1.2	0.1022	0.213	1.2	0.0302	0.0822
1.3	0.0478	0.121	1.3	0.0067	0.0436
1.4	0.019	0.019	1.343	0.0168	0.0168

APPENDIX II (cont'd)

Stator 2

Root (9.96 in. radius)
LER = 0.07 in. TER = 0.016 in.
Stagger angle = 31.0 deg.

x	y_p	y_s
0	0.072	0.072
0.05	0.0038	0.170
0.10	0.006	0.229
0.20	0.044	0.311
0.30	0.076	0.3605
0.40	0.102	0.388
0.50	0.121	0.3955
0.60	0.1345	0.3845
0.70	0.142	0.3565
0.80	0.144	0.320
0.90	0.1395	0.283
1.00	0.129	0.244
1.10	0.112	0.202
1.20	0.089	0.159
1.30	0.0605	0.114
1.40	0.0245	0.065
1.48	0.0175	0.0175

Tip (14.26 in. radius)
LER = 0.10 in. TER = 0.016 in.
Stagger angle = 22.1 deg.

x	y_p	y_s
0	0.098	0.098
0.05	0.0145	0.190
0.10	0	0.2365
0.20	0.029	0.309
0.30	0.060	0.361
0.40	0.0865	0.398
0.50	0.1075	0.422
0.60	0.124	0.4318
0.70	0.136	0.430
0.80	0.1445	0.417
0.90	0.148	0.3895
1.00	0.1475	0.353
1.10	0.142	0.3145
1.20	0.1325	0.275
1.30	0.1185	0.235
1.40	0.100	0.192
1.50	0.078	0.1498
1.60	0.050	0.1045
1.70	0.017	0.058
1.76	0.0185	0.0185

APPENDIX II (cont'd)

Rotor 2 (datum design)

Root (9.835 in. radius) LER = 0.0375 in. TER = 0.016 in. Stagger angle = 9.5 deg.			Tip (14.41 in. radius) LER = 0.025 in. TER = 0.016 in. Stagger angle = 37.2 deg.		
x	y_p	y_s	x	y_p	y_s
0	0.038	0.038	0	0.022	0.022
0.05	0.0025	0.114	0.05	0.0115	0.082
0.10	0.0285	0.169	0.10	0.042	0.121
0.20	0.0745	0.252	0.20	0.0885	0.177
0.30	0.112	0.312	0.30	0.1205	0.215
0.40	0.143	0.354	0.40	0.139	0.236
0.50	0.1655	0.381	0.50	0.1458	0.2425
0.60	0.182	0.395	0.60	0.143	0.236
0.70	0.1925	0.396	0.70	0.1378	0.226
0.80	0.1965	0.384	0.80	0.131	0.2135
0.90	0.1935	0.361	0.90	0.123	0.200
1.0	0.185	0.331	1.0	0.113	0.184
1.1	0.170	0.2975	1.1	0.101	0.167
1.2	0.148	0.258	1.2	0.088	0.149
1.3	0.120	0.2138	1.3	0.073	0.128
1.4	0.083	0.163	1.4	0.0565	0.1065
1.5	0.044	0.106	1.5	0.038	0.082
1.6	0.0035	0.0438	1.6	0.0185	0.0565
1.625	0.017	0.017	1.70	0.012	0.012

APPENDIX II (cont'd)

Rotor 1 (new design)

Root (10.43 in. radius)
LER = 0.018 in. TER = 0.014 in.
Stagger angle = 17.9 deg.

x	y_p	y_s
0	0.0455	0.0455
0.05	0.003	0.175
0.1	0.022	0.2405
0.2	0.0855	0.325
0.3	0.139	0.378
0.4	0.1765	0.4145
0.5	0.199	0.428
0.6	0.212	0.4245
0.7	0.219	0.4170
0.8	0.2158	0.377
0.9	0.200	0.338
1.0	0.177	0.293
1.1	0.145	0.240
1.2	0.107	0.1805
1.3	0.0622	0.1160
1.4	0.0115	0.0490
1.438	0.0145	0.0145

Tip (13.79 in. radius)
LER = 0.008 in. TER = 0.012 in.
Stagger angle = 32.8 deg.

x	y_p	y_s
0	0.011	0.011
0.05	0.0265	0.1095
0.1	0.065	0.1665
0.2	0.138	0.242
0.3	0.1855	0.289
0.4	0.2125	0.312
0.5	0.225	0.3195
0.6	0.223	0.3095
0.7	0.2125	0.288
0.8	0.1925	0.257
0.9	0.163	0.217
1.0	0.126	0.170
1.1	0.0795	0.117
1.2	0.029	0.0605
1.265	0.0125	0.0125

APPENDIX II (cont'd)

Rotor 2 (new design)

Root (9.92 in. radius) LER = 0.015 in. TER = 0.011 in. Stagger angle = 12.9 deg.			Tip (14.31 in. radius) LER = 0.005 in. TER = 0.008 in. Stagger angle = 36.8 deg.		
x	y_p	y_s	x	y_p	y_s
0	0.0178	0.0178	0	0.005	0.005
0.05	0.0069	0.1235	0.05	0.0218	0.0598
0.1	0.0295	0.1745	0.10	0.493	0.0980
0.2	0.0790	0.2477	0.2	0.0963	0.1538
0.3	0.1185	0.2985	0.3	0.1315	0.1935
0.4	0.1479	0.3312	0.4	0.1560	0.2208
0.5	0.1685	0.3505	0.5	0.1713	0.2378
0.6	0.1797	0.3567	0.6	0.1793	0.2453
0.7	0.1873	0.3503	0.7	0.1835	0.2463
0.8	0.1895	0.3345	0.8	0.1810	0.2390
0.9	0.1850	0.3128	0.9	0.1748	0.2255
1.0	0.1752	0.2850	1.0	0.1640	0.2095
1.1	0.1603	0.2528	1.1	0.1490	0.1895
1.2	0.1405	0.2155	1.2	0.1300	0.1643
1.3	0.1143	0.1743	1.3	0.1088	0.1373
1.4	0.0835	0.1313	1.4	0.0848	0.1095
1.5	0.0490	0.0845	1.5	0.0548	0.0765
1.6	0.0100	0.0360	1.6	0.0215	0.0405
1.637	0.0113	0.0113	1.67	0.008	0.008

APPENDIX III

Test data - Series 1

	N	M	L	T_1	T_5	P_1	P_{10}	P_{11}	P_{20}	P_{21}	P_{30}	P_{31}	P_{40}	P_{5A}	P_{5B}	P_{5C}	P_{5D}	P_{5E}	P_{50}	P_{51}	P_{5calc}	α_5
1	2575	44.69	617	386.8	357.6	43.33	40.20	40.52	33.78	32.33	30.23	31.96	29.61	30.44	30.53	30.76	30.69	30.84	29.49	29.54	30.61	- 6.9
2	2517	50.45	795	383.1	350.0	46.44	42.87	43.15	34.65	32.73	30.13	32.46	29.45	30.52	30.60	31.03	31.08	31.16	29.34	29.42	30.74	3.7
3	2584	59.42	1126	384.2	343.7	52.55	47.97	48.46	36.86	33.93	30.13	33.4	29.24	30.30	30.73	31.37	31.57	31.68	29.6	29.11	30.96	8.47
4	2534	65.92	1384	384.8	340.1	57.57	52.36	52.93	39.01	35.33	30.34	34.56	39.05	30.48	30.99	31.79	31.77	32.28	28.73	28.82	31.22	14.05
5	2571	74.50	1746	385.8	336.0	64.21	58.30	58.96	42.51	37.83	31.09	36.5	28.82	30.49	31.27	32.37	32.57	33.31	28.33	28.37	31.59	17.2
6	2571	83.65	2136	386.6	332.0	72.4	65.67	66.42	46.91	41.36	32.66	39.3	28.86	31.0	31.63	32.97	33.73	34.74	27.96	27.82	32.21	21.45
7	2579	93.63	2564	387.5	328.2	80.29	73.40	74.19	51.91	45.66	35.02	42.9	29.47	31.44	32.22	33.94	34.17	36.39	27.58	27.13	33.20	25.28
8	3936	49.83	600	386.6	349.2	47.04	43.59	44.00	35.68	34.15	30.66	32.35	29.32	30.68	30.55	30.58	30.50	30.67	29.06	28.91	30.59	-23.9
9	3933	56.36	816	391.4	345.2	51.53	47.43	47.9	37.3	35.41	30.74	33.21	29.1	30.51	30.76	30.87	30.78	30.90	28.76	28.72	30.57	-15.77
10	3937	63.44	1066	393.2	339.4	56.79	52.08	52.64	39.47	37.05	30.84	34.35	28.87	30.53	30.83	31.11	30.89	31.10	28.52	28.55	30.86	-10.23
11	3942	68.84	1267	396.3	336.4	61.26	56.07	56.88	41.6	38.38	30.88	35.35	28.85	30.56	30.56	31.22	31.11	31.56	28.29	28.4	30.91	- 7.3
12	3939	74.60	1487	395.2	333.1	66.02	60.32	60.99	44.10	40.85	31.19	36.75	28.8	30.54	30.68	31.37	31.75	32.01	28.10	28.25	31.13	- 4
13	3490	82.37	1797	400.0	328.8	72.77	66.49	67.21	48.05	44.22	31.74	36.95	28.72	30.44	30.86	31.97	32.67	33.08	27.69	27.9	31.2	4.7
14	3944	94.95	2319	401.9	322.3	83.96	76.63	77.5	54.97	50.48	34.1	43.28	29.25	30.86	31.57	33.17	33.31	33.77	26.86	27.12	32.11	12.92
15	3919	103.01	2604	398.7	316.7	90.85	82.92	83.89	59.59	54.54	35.81	46.54	30.26	31.17	32.24	34.13	34.01	36.15	26.74	26.8	32.91	15.82
16	3927	111.24	2956	402.7	315.7	98.26	89.77	90.70	64.16	58.97	39.47	50.24	31.64	31.89	33.07	35.00	34.93	37.26	26.32	26.12	33.87	19.6
17	3927	119.12	3242	401.4	311.6	104.86	95.66	96.76	68.56	63.04	41.77	53.61	32.71	32.84	34.04	36.14	36.08	38.53	26.16	25.63	35.07	22.4
18	3924	125.07	3455	402	311.2	110.35	100.71	101.88	72.01	67.54	44.17	56.41	34.96	33.85	35.17	37.43	37.43	40.17	26.25	25.43	36.20	23.77
19	4459	49.70	514	383.5	346.1	47.32	43.32	44.18	36.43	34.79	31.07	32.54	29.73	31.3	31.39	31.32	31.03	31.00	29.53	29.14	31.14	-32.12
20	4454	57.93	747	384.2	337.5	52.79	48.45	48.93	38.48	36.26	31.41	33.66	29.33	31.27	31.02	31.10	30.99	31.22	29.10	28.92	31.11	-24.35
21	4604	63.73	918	397.7	342	57.09	52.42	52.95	40.17	38	31.47	34.46	29.49	30.95	31.04	31.10	31.13	31.26	28.69	28.58	30.98	-18.55
22	4604	70.37	1183	398.3	334.9	63.12	57.74	58.37	43.20	40.50	31.82	35.96	29.07	31.02	31.27	31.44	31.46	31.80	28.32	28.36	31.11	-13.55
23	4600	80.26	1538	399.5	327.2	71.43	65.31	66.06	47.97	44.65	32.69	38.55	29.03	31.06	30.87	31.73	31.66	32.47	27.92	28.09	31.45	- 7.67
24	4608	89.22	1857	400.8	321.2	79.55	72.61	73.44	52.98	41.95	34.20	41.60	29.27	31.07	31.10	31.84	32.30	33.43	27.54	27.8	31.87	3.9
25	4604	96.39	2134	402.3	318.2	85.88	78.38	79.28	57.07	52.96	36.00	44.42	29.67	31.03	31.59	32.62	33.57	34.39	27.19	27.44	32.26	5.7
26	4608	107.8	2565	403.5	312.2	95.92	87.57	88.57	63.63	59.09	39.56	49.34	31.07	32.08	32.15	33.58	34.32	35.89	26.41	26.53	33.01	12.2
27	5243	60.66	732	390.2	339.6	55.44	50.94	51.46	39.72	37.71	31.57	33.81	29.32	31.62	31.55	31.40	31.35	31.33	28.85	28.40	31.21	-29.7
28	5253	69.41	1027	401	336.7	62.76	57.55	58.17	43.39	40.97	32.17	35.86	29.12	31.58	30.98	31.09	31.26	31.51	28.25	28.05	31.14	-21.53
29	5242	77.18	1257	395	327.4	68.97	63.11	63.82	46.90	44.05	32.92	37.55	29.27	31.23	31.47	31.47	31.82	32.06	27.98	27.93	31.30	-15.46

APPENDIX III (cont'd)

Test data - Series 1 (cont'd)

	N	M	L	T_1	T_5	P_1	P_{10}	P_{11}	P_{20}	P_{21}	P_{30}	P_{31}	P_{40}	P_{5A}	P_{5B}	P_{5C}	P_{5D}	P_{5E}	P_{50}	P_{51}	P_{5calc}	α_5
30	5243	86.75	1607	401.7	321.7	77.51	70.88	71.69	52.34	48.99	34.64	40.65	29.30	31.32	31.23	31.97	32.25	32.94	27.33	27.46	31.52	-10.3
31	5253	92.35	1751	394.3	312.3	81.85	74.8	75.63	55.22	51.51	35.38	42.44	29.64	31.42	31.14	31.96	32.46	33.5	27.17	27.39	31.67	- 7.93
32	5263	97.65	1948	400.2	314.3	87.12	79.68	80.65	58.66	54.94	37.85	45.07	30.25	31.6	31.09	32.11	32.89	34.06	27.08	27.34	32.22	- 5.05
33	5253	101.03	2081	402.2	312.3	90.21	82.5	83.41	60.71	56.81	39.08	46.52	30.48	31.4	31.29	32.16	33.21	34.59	26.83	27.12	32.37	4
34	5243	105.92	2213	395.6	305	94.02	85.88	86.63	63.49	59.07	40.14	48.44	31.05	31.36	31.53	32.55	33.75	35.22	26.57	26.92	32.60	4.5
35	5253	112.10	2460	401.7	305.6	100.02	91.46	92.49	67.23	62.96	43.03	51.45	32.29	31.82	32.44	33.30	34.86	36.49	26.25	26.56	33.17	7.85
36	5258	122.31	2796	402.2	301.7	109.05	99.74	100.85	73.31	68.66	47.00	56.11	34.84	33.71	33.85	34.84	36.13	38.25	25.74	25.92	34.27	12.7

APPENDIX III (cont'd)

Test data - Series 2

	N	M	L	T_1	T_5	P_1	P_{10}	P_{11}	P_{20}	P_{21}	P_{30}	P_{31}	P_{5A}	P_{5B}	P_{5C}	P_{5D}	P_{5E}	P_{50}	P_{51}	P_{5calc}	α_5
1	3863	37.23	263	386.8	364.3	38.14	35.75	35.96	30.94	29.91	28.63	28.48	30.03	30.15	30.09	30.17	29.9	28.71	28.83	29.97	7.95
2	3871	41.14	337	385.1	358.7	40.02	37.16	37.46	31.39	29.98	28.43	28.31	30.18	30.35	30.32	30.34	30.04	28.51	28.69	30.12	13.0
3	3865	45.91	438	386.3	355.5	42.60	39.30	39.58	32.11	30.08	28.28	28.18	30.35	30.77	30.81	30.71	30.37	28.35	28.55	30.42	18.1
4	3885	47.83	487	388.6	355.9	43.91	40.36	40.67	32.09	30.21	28.16	28.08	30.48	31.06	31.08	30.94	30.54	28.26	28.47	30.58	20.2
5	3863	52.20	598	388.4	351.3	46.74	42.77	43.12	32.84	30.51	28.02	27.78	30.74	31.79	31.84	31.54	30.84	28.13	28.32	31.01	24.5
6	4692	38.74	241	392.5	369.5	39.66	37.14	37.39	31.93	30.93	29.25	28.9	30.61	30.84	30.81	30.76	30.41	29.27	29.33	30.60	- 5.2
7	4679	43.66	333	390.9	361.6	42.20	39.21	39.52	32.0	31.0	29.01	28.73	30.77	30.96	30.93	31.00	30.69	29.03	29.21	30.73	4.9
8	4659	48.11	421	386.1	352.5	44.27	40.89	41.24	32.84	31.14	28.59	28.41	30.8	31.00	30.94	31.08	30.72	28.66	28.93	30.76	10.62
9	4588	51.60	489	376.9	341.3	46.30	42.56	42.91	33.67	31.59	28.50	28.42	31.14	31.38	31.34	31.53	31.22	28.69	29.02	31.08	12.8
10	4659	54.85	574	383.5	343.7	48.74	44.63	45.01	34.44	32.02	28.31	28.32	31.31	31.74	31.81	31.84	31.54	28.5	28.88	31.32	15.85
11	4608	57.92	643	381	339.0	50.86	46.45	46.88	35.22	32.42	28.19	28.16	31.55	32.0	32.11	32.20	31.98	28.37	28.78	31.60	19.5
12	4584	61.33	720	379.5	334.4	53.31	48.61	49.1	36.37	33.22	28.01	27.99	31.47	32.26	32.71	32.77	32.42	28.21	28.67	31.98	22.7
13	4592	66.27	842	378.6	329.7	57.29	52.22	52.68	38.59	34.92	27.85	27.76	32.22	33.28	33.53	33.92	33.43	28.1	28.63	32.75	27.0
14	4627	67.55	902	387.3	333.8	59.04	53.78	54.27	39.44	35.74	27.35	27.01	32.55	33.51	33.70	33.82	33.40	27.56	28.03	32.77	29.3
15	5212	38.40	207	389.1	367.1	39.39	37.02	37.25	31.81	30.75	29.25	28.61	30.69	30.79	30.82	30.58	30.32	29.24	29.19	30.56	-15.1
16	5217	45.45	328	388.5	357.9	43.05	39.93	40.25	32.78	31.31	28.87	28.45	30.66	30.96	30.97	30.93	30.53	28.87	29.03	30.83	- 3.8
17	5163	50.29	438	388.9	351.7	46.20	42.60	42.95	33.56	31.75	28.50	28.25	30.85	31.06	31.04	31.19	30.82	28.57	28.87	30.81	4.7
18	5202	53.86	509	387.9	347.4	48.31	44.42	44.81	34.26	32.11	28.20	28.05	30.99	31.25	31.21	31.43	31.07	28.34	28.71	30.97	9.5
19	5148	58.39	627	389.3	343.8	51.65	47.37	47.80	35.43	33.11	27.93	27.91	31.43	31.64	31.72	31.91	31.76	28.08	28.58	31.35	15.8
20	5143	60.60	676	388.1	340.9	53.30	48.83	49.29	36.46	33.71	27.78	27.78	31.41	31.86	31.97	32.08	31.94	27.95	28.49	31.54	18.2
21	5153	64.80	775	389.1	337.5	56.67	51.86	52.36	38.41	35.35	27.54	27.55	31.89	32.46	32.47	32.55	32.74	27.81	28.40	32.12	22.85
22	5148	67.59	843	388.8	335.1	59.19	54.15	54.66	39.81	36.58	27.44	27.38	32.31	32.98	33.13	33.22	33.33	27.74	28.34	32.55	25.08
23	5133	70.46	915	389.7	332.9	61.59	56.35	56.88	41.36	37.91	27.44	27.18	32.91	33.68	33.76	34.04	34.26	27.72	28.33	33.09	27.05
24	5153	72.56	970	387.6	328.2	63.6	57.97	58.5	42.85	38.87	26.94	26.40	32.8	33.69	33.9	35.26	34.31	27.15	27.73	33.15	29.25
25	5163	77.84	1097	387.8	325.3	68.17	62.14	62.66	45.68	41.63	27.07	25.87	33.83	35.08	35.27	35.83	35.62	27.11	27.6	34.42	32.65
26	5163	83.61	1225	388.4	322.9	73.17	66.66	67.3	48.9	44.6	27.24	25.33	35.65	36.43	37.21	37.5	37.21	27.08	27.4	35.89	35.05
27	5607	48.76	365	375.8	341.4	44.18	40.82	41.17	32.81	31.16	28.08	27.63	30.14	30.45	30.45	30.44	29.93	28.08	28.27	30.16	- 7.25
28	5619	56.32	527	374.9	331.5	49.31	45.27	45.66	34.58	32.3	27.45	27.23	30.44	30.61	30.62	30.78	30.58	27.58	27.98	30.38	7.7
29	5602	62.73	667	373.3	324.0	54.12	49.58	49.97	36.86	34.16	26.93	27.00	31.00	31.03	31.08	31.53	31.56	27.17	27.79	30.85	14.75
30	5613	67.00	769	377.0	323.0	57.88	53.0	53.52	39.28	36.16	26.70	26.70	31.49	31.65	31.68	32.00	32.41	26.86	27.65	31.35	19.43
31	5613	72.17	893	378.0	320	62.49	57.18	57.72	42.13	38.80	26.54	26.3	32.66	32.88	32.71	32.58	33.37	26.75	27.51	32.28	25.18
32	5637	94.33	1354	382.0	312.6	82.04	74.79	75.55	55.34	50.62	27.54	25.06	37.44	39.12	39.35	39.56	39.99	27.06	27.64	38.19	35.8

APPENDIX III (cont'd)

Test data - Series 3

	N	M	L	T_1	T_5	P_1	P_{10}	P_{11}	P_{20}	P_{21}	P_{30}	P_{31}	P_{40}	P_{5A}	P_{5B}	P_{5C}	P_{5D}	P_{5E}	P_{50}	P_{51}	P_{5calc}	σ_5
1	4667	5.65	750	400.5	351.6	52.98	48.77	49.45	38.88	-	32.08	33.36	29.61	30.85	30.77	30.86	30.99	31.16	28.9	28.79	30.82	-20.44
2	4651	64.91	1018	401.3	342.7	58.96	54.22	54.97	41.68	-	32.6	34.66	29.74	30.92	30.83	30.95	31.26	31.34	28.53	28.57	30.95	-13.8
3	4655	72.45	1288	402	335.5	65.24	59.62	60.69	44.75	-	33.46	35.85	29.92	30.87	31.10	31.34	31.83	32.01	28.26	28.45	31.25	- 7.25
4	4655	83.17	1662	403.8	328.1	74.03	67.67	68.64	49.45	-	34.88	38.55	30.27	30.73	30.90	31.67	32.07	32.76	27.81	28.15	31.62	2.5
5	4655	90.44	1936	405.4	323.9	80.43	73.57	74.67	53.18	-	36.92	40.83	30.45	30.77	31.01	31.85	32.55	33.34	27.4	27.77	31.93	3.43
6	4663	97.27	2203	406.7	319.8	86.18	78.72	79.98	56.36	-	39.05	43.35	30.60	31.28	31.45	32.34	33.38	34.03	26.96	27.35	32.27	7.7
7	4667	105.43	2510	407.2	315.5	93.58	85.55	86.86	61.45	-	41.98	46.6	31.61	31.51	32.1	33.27	34.6	35.14	26.41	26.76	32.81	11.2
8	4667	111.69	2741	408.4	312.5	98.99	90.47	91.96	64.80	-	44.22	49.24	32.55	31.86	32.72	34.11	35.8	36.13	26.03	26.31	33.43	14.3
9	5233	56.23	597	387.4	343.9	52.42	48.39	48.82	39.14	37.45[x]	32.58	33.11	30.03	31.33	31.45	31.27	31.25	31.2	29.39	28.91	31.72	-36.68
10	5284	65.18	885	398.2	337.5	59.25	54.32	54.85	42.35	-	33.35	34.67	30.03	31.37	31.29	31.35	31.54	31.52	28.8	28.59	31.33	-23.93
11	5315	69.25	1072	407.2	342.6	63.15	57.97	58.68	43.98	41.53[x]	33.40	35.48	29.63	31.01	30.6	30.77	31.03	31.44	28.15	28.08	30.99	-13.0
12	5362	83.19	1529	410.5	331.8	75.08	68.69	69.62	50.65	47.43[x]	35.9	39.06	30.23	31.11	31.31	31.51	32.3	32.52	27.56	27.81	31.48	- 8.5
13	5389	89.77	1770	416.7	330.8	81.32	74.37	75.41	54.38	50.85[x]	37.94	41.42	30.65	31.08	31.27	31.84	32.46	33.25	27.22	27.65	31.82	- 4.0
14	5325	102.74	2156	406.4	315.7	91.70	83.94	85.77	61.72	-	42.27	46.16	31.83	31.6	31.8	32.69	33.39	34.85	27.00	27.49	32.80	4.6
15	5310	106.9	2297	406.3	311	95.59	87.12	-	64.53	-	43.93	47.70	32.19	31.44	31.58	32.83	33.76	35.25	26.47	27.00	33.13	6.0
16	5310	114.59	2514	399.3	302.4	101.54	92.54	93.36	67.49	64.47[x]	46.78	50.75	33.43	31.94	32.15	33.16	34.35	35.87	26.31	26.84	33.36	9.41
17	5315	126.23	2874	398.8	296.8	111.35	101.34	102.68	74.23	71.04[x]	51.38	55.55	35.73	32.97	33.56	34.5	35.99	37.36	25.78	26.24	34.62	12.5

[x]One tapping only

APPENDIX III (cont'd)

Test data - Series 4

	N	M	L	T_1	T_5	P_1	P_{10}	P_{11}	P_{20}	P_{21}	P_{30}	P_{31}	P_{5A}	P_{5B}	P_{5C}	P_{5D}	P_{5E}	P_{50}	P_{51}	P_{5calc}	α_5
1	4361	44.37	353	380	351.2	42.17	39.25	-	32.88	-	29.24	28.46	30.41	30.63	30.57	30.78	30.40	28.98	29.09	30.48	3.8
2	4627	51.12	497	381.2	345.7	46.20	42.56	-	34.01	-	28.97	28.10	30.88	31.12	30.94	31.01	30.69	28.67	28.88	31.08	13.8
3	4643	57.13	633	381.6	340.4	50.12	46.05	-	35.35	-	28.81	27.83	31.18	31.75	31.74	31.75	30.80	28.45	28.73	31.63	19.77
4	4647	62.11	755	381.8	336.1	53.81	49.32	-	36.68	-	28.68	27.48	31.47	32.37	32.35	32.67	31.18	28.25	28.54	32.18	23.85
5	4655	65.60	843	382.0	333.2	56.50	50.68	-	37.80	-	28.63	27.26	31.77	33.01	32.9	32.89	31.61	28.16	28.46	32.73	26.9
6	4647	68.50	916	382.6	331	58.88	53.81	-	38.88	-	28.61	27.07	32.10	33.64	33.51	33.74	32.06	28.08	28.38	33.22	28.88
7	5177	53.03	501	382.8	344	47.64	43.8	-	34.57	-	28.67	27.71	30.75	30.73	30.65	30.91	30.55	28.26	28.39	30.83	11.45
8	5217	56.91	618	397.4	350.3	51.00	46.83	-	35.62	-	28.44	27.42	30.92	31.32	31.14	31.16	30.56	28.07	28.53	31.23	15.75
9	5197	63.21	736	384.7	335.6	55.10	50.41	-	37.90	-	28.55	27.40	31.51	32.08	32.31	32.00	31.07	28.13	28.64	32.00	19.92
10	5202	68.60	872	387.8	333	59.57	54.49	-	39.58	-	28.45	27.07	32.31	32.93	32.89	33.23	31.78	27.96	28.53	32.80	24.3
11	5228	69.52	925	396.1	337.7	60.91	55.87	-	40.05	-	28.12	26.62	31.84	33.01	32.98	33.42	31 39	27.61	28.22	32.83	25.64
12	5212	74.27	1015	389.1	330	64.47	59.03	-	42.27	-	28.39	26.62	32.57	34.03	33.96	34.47	32.30	27.83	28.30	33.75	27.88
13	5212	78.00	1098	388.5	327.9	67.47	61.73	-	44.03	-	28.44	26.30	32.94	34.80	34.71	35.16	32.89	27.76	28.19	34.44	29.52
14	5294	81.54	1212	400 3	335	71.56	65.41	-	46.34	-	28.21	25.50	33.61	35.98	35.74	36.13	33.61	27.48	27.72	35.12	30.65
15	5726	55.62	521	387	344.1	49.74	45.64	-	35.55	-	28.71	27.63	30.76	30.89	30.89	31.20	30.70	28.31	28.70	31.05	6.3
16	5720	61.73	666	389.1	337.7	54.32	49.67	-	37.38	-	28.43	27.28	31.83	31.37	31.19	31.53	31.22	27.97	28.50	31.55	14.54
17	5708	67.73	804	388.3	332.6	59.06	53.95	-	39.66	-	28.25	26.95	32.33	32.18	32.04	32.12	32.09	27.73	28.32	32.18	19.5
18	5732	73.49	934	388	328.3	63.75	58.12	-	42.18	-	28.16	26.53	32.79	33.06	32.97	32.90	32.56	27.50	28.13	32.93	22.85
19	5714	79.92	1090	388.5	324.8	69.54	63.52	-	45.63	-	28.10	25.90	33.09	34.42	34.35	34.54	33.32	27.39	27.88	34.22	26.24

FIG. 1

DATUM TURBINE
ANNULUS DIMENSIONS - INCHES

STATION	C - C	D - D	E - E	F - F	G - G
OUTER DIA	26 92	27 60	28·08	28 54	29·07
INNER DIA	21 36	20 94	20 32	19 88	19 25

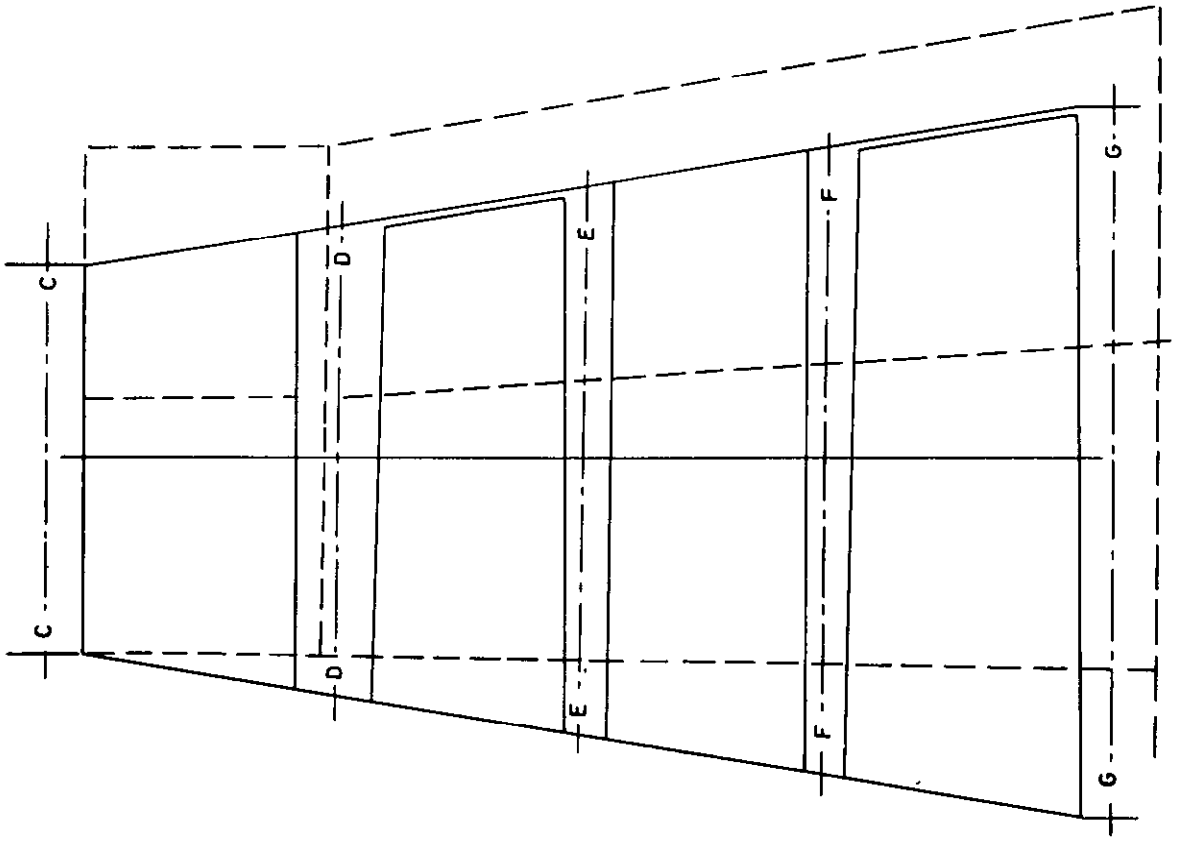

DATUM TURBINE		REFERENCE TURBINE
3 8	STAGE 1 $2K_p\Delta T/U^2$	3 19
0 95	V_a/U	0 78
15°	α_3	15°
2·67	STAGE 2 $2K_p\Delta T/U^2$	2 70
1 10	V_a/U	0 965
−1°	α_3	1°

DESIGN PARAMETERS FOR DATUM AND REFERENCE TURBINES.

ROTOR BLADE THICKNESS DISTRIBUTIONS.

SEMI-ORDINATES AS PERCENTAGE OF BLADE CHORD

STATION ON CAMBER LINE	1·25	2·5	5	10	20	30 ·	40	50	60	70	80	90
ROOT SECTION SEMI-ORDINATES	1·375	1·940	2·675	3 600	4·550	4·950	4 820	3 980	3 080	2 260	1 540	0 970
TIP SECTION SEMI-ORDINATES	1 375	1 940	2·675	3·600	4·550	4·950	4·900	4·175	3·345	2·620	1·975	1·510

	LEADING EDGE RADIUS	TRAILING EDGE RADIUS ·
ROOT	8 %o t_m	6 %o t_m
TIP	8 %o t_m	12 %o t_m

(RADII EXPRESSED AS A %o AGE OF MAXIMUM THICKNESS t_m)

FIG. 2

FIG. 3

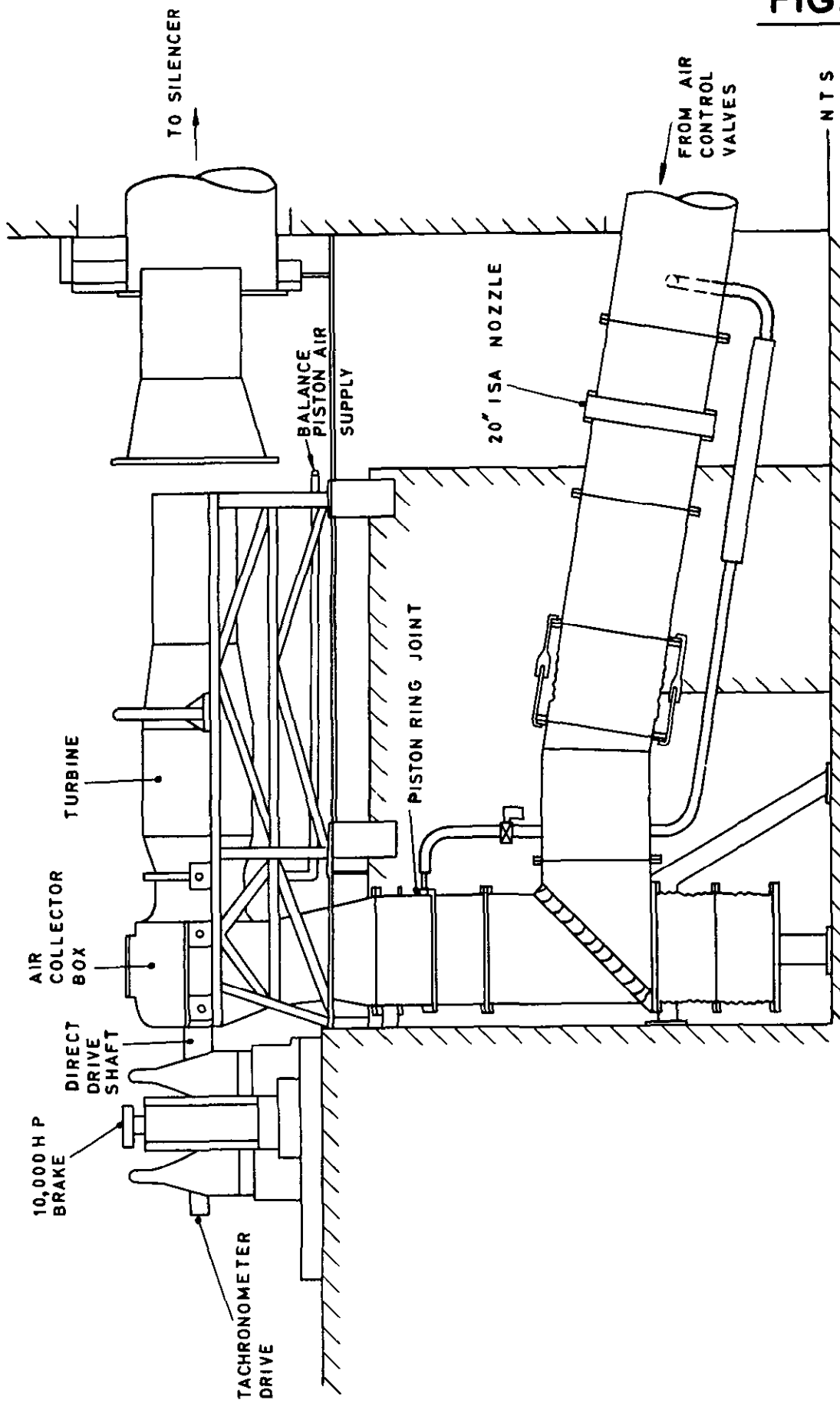

GENERAL ARRANGEMENT OF TURBINE TEST FACILITY.

FIG. 4

DIAGRAM OF TURBINE INLET SECTION

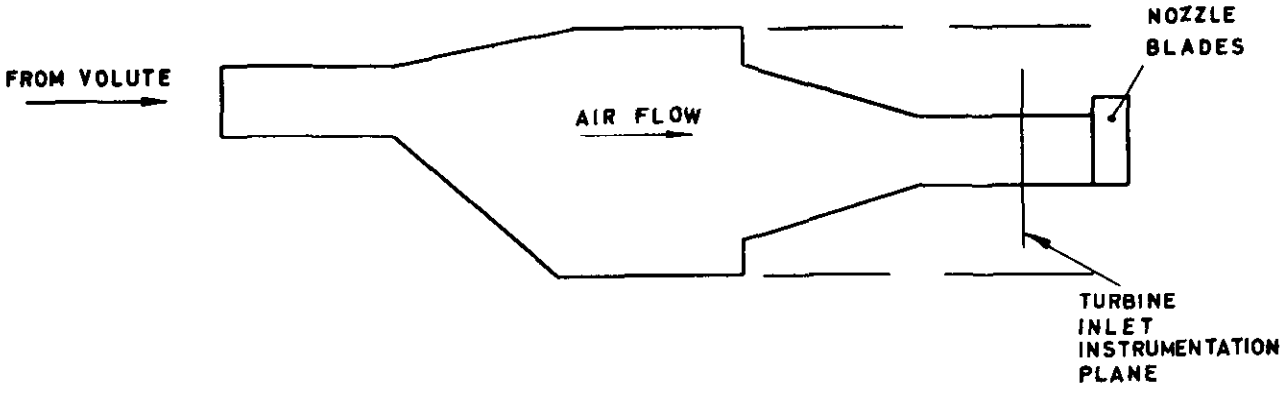

RADIAL DISTRIBUTIONS AT INLET

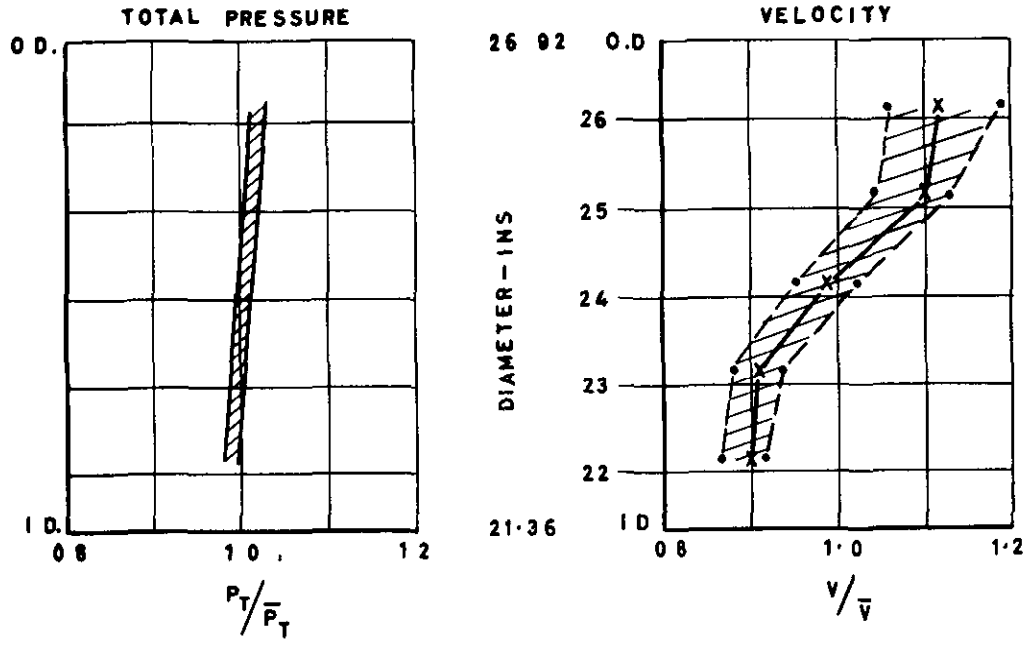

TURBINE INLET CONDITIONS.

FIG. 5

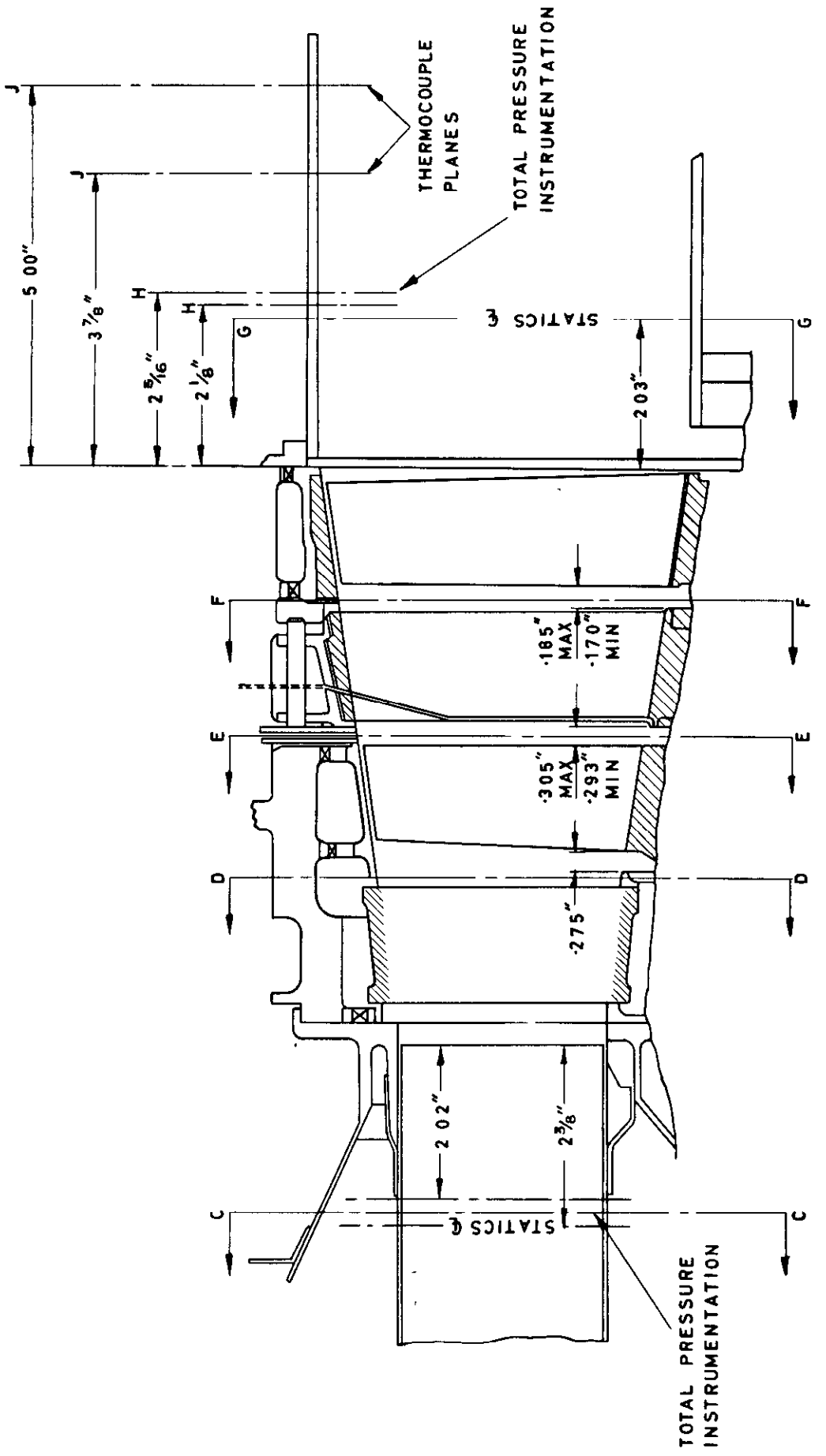

RADIAL LOCATION OF EXIT TOTAL PRESSURE PROBES

READING	P_{S_A}	P_{S_B}	P_{S_C}	P_{S_D}	P_{S_E}
DIAMETER	28 22	26·47	24 58	22·54	20 30

TWO STAGE BLADE ANNULUS.

FIG. 6

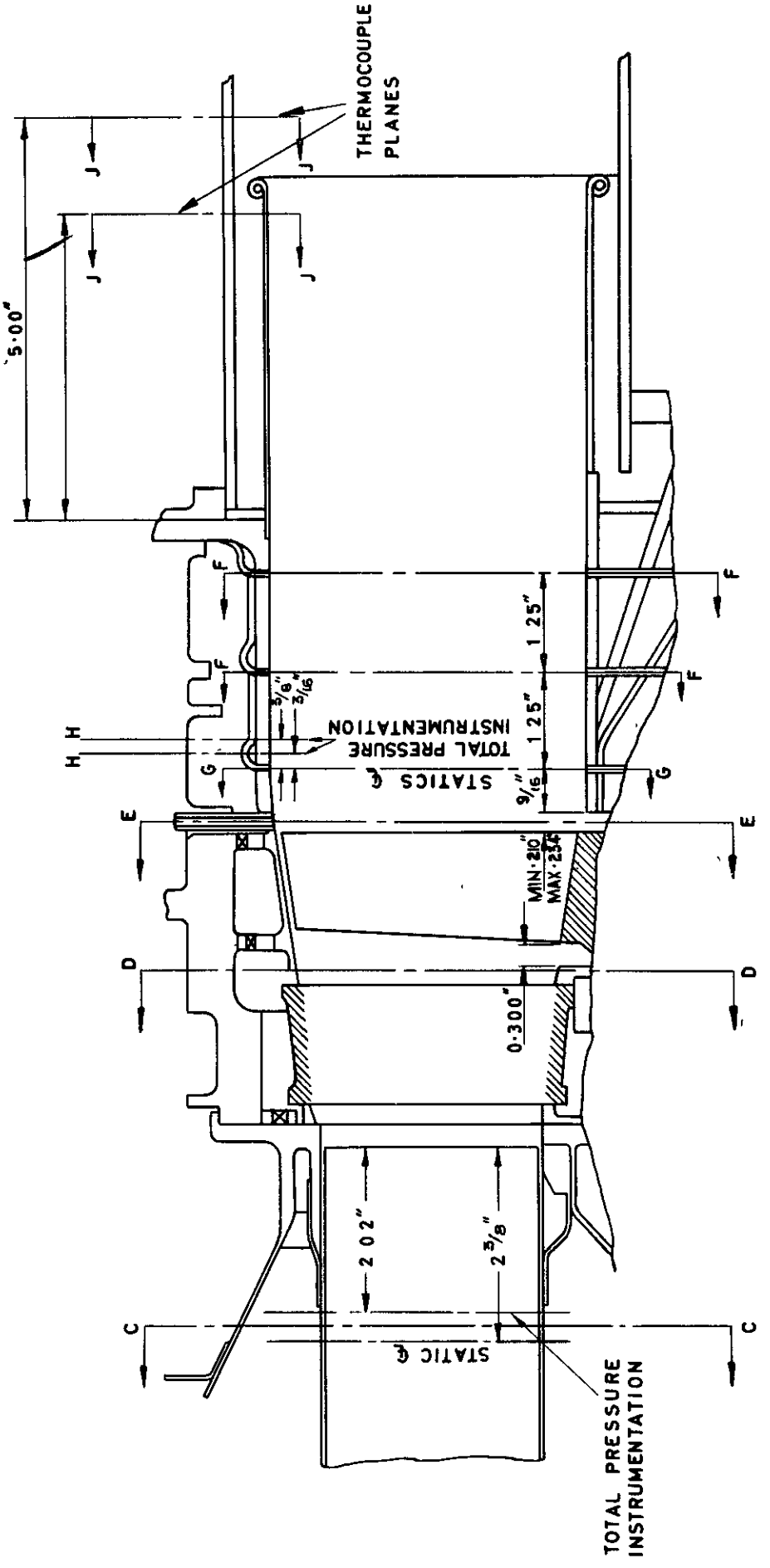

RADIAL LOCATION OF EXIT TOTAL PRESSURE PROBES

READING	P_{5A}	P_{5B}	P_{5C}	P_{5D}	P_{5E}
DIAMETER	27 52	25 97	24 43	22·79	21 02

SINGLE STAGE BLADE ANNULUS.

FIG. 7

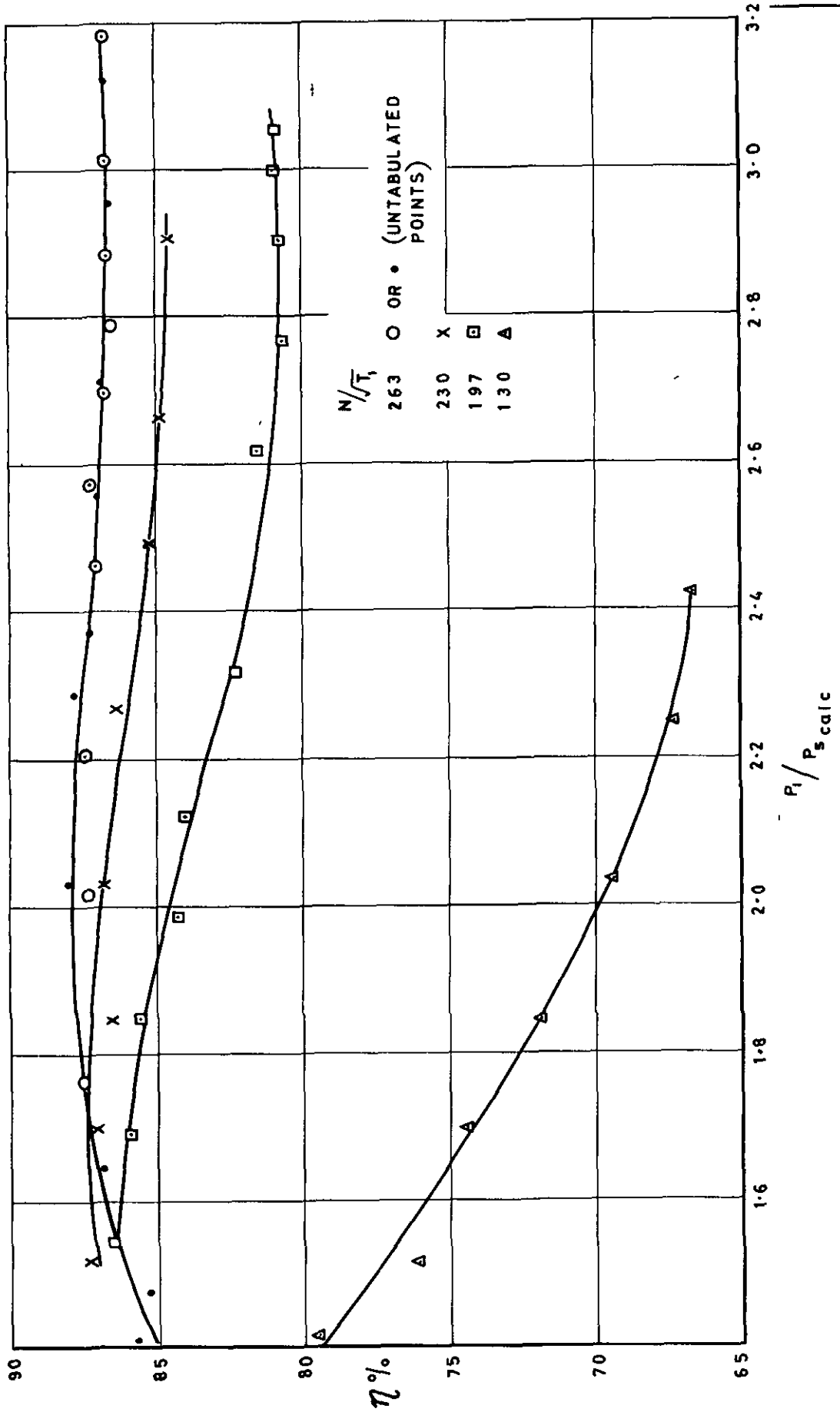

SERIES 1 (EFFICIENCY – $P_{5\ CALC.}$)

TWO STAGE – DATUM BLADES.

FIG. 8

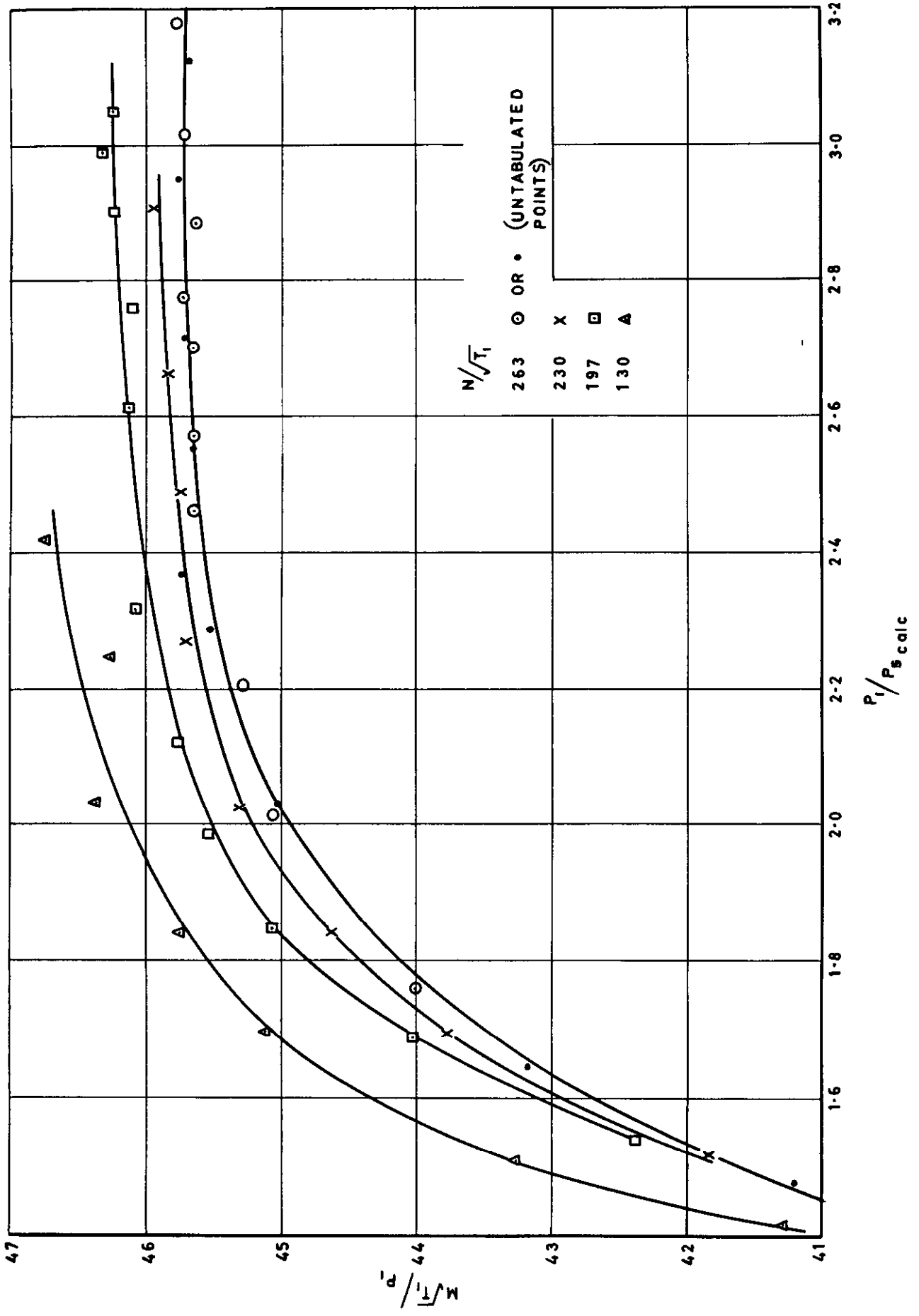

SERIES I (FLOW)
TWO STAGE - DATUM BLADES.

FIG. 9

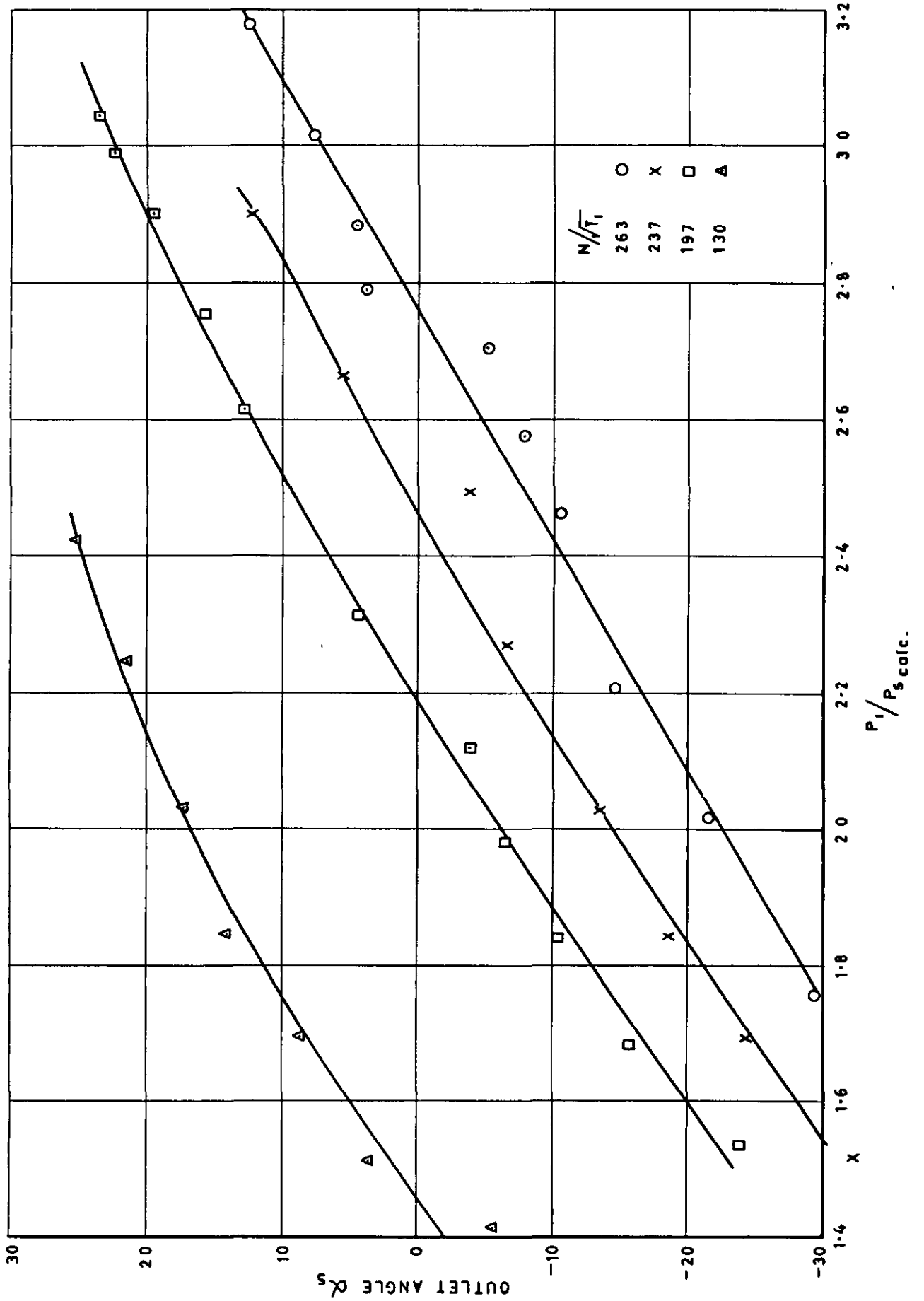

SERIES I (EXIT SWIRL)
TWO STAGE-DATUM BLADES.

FIG. 10

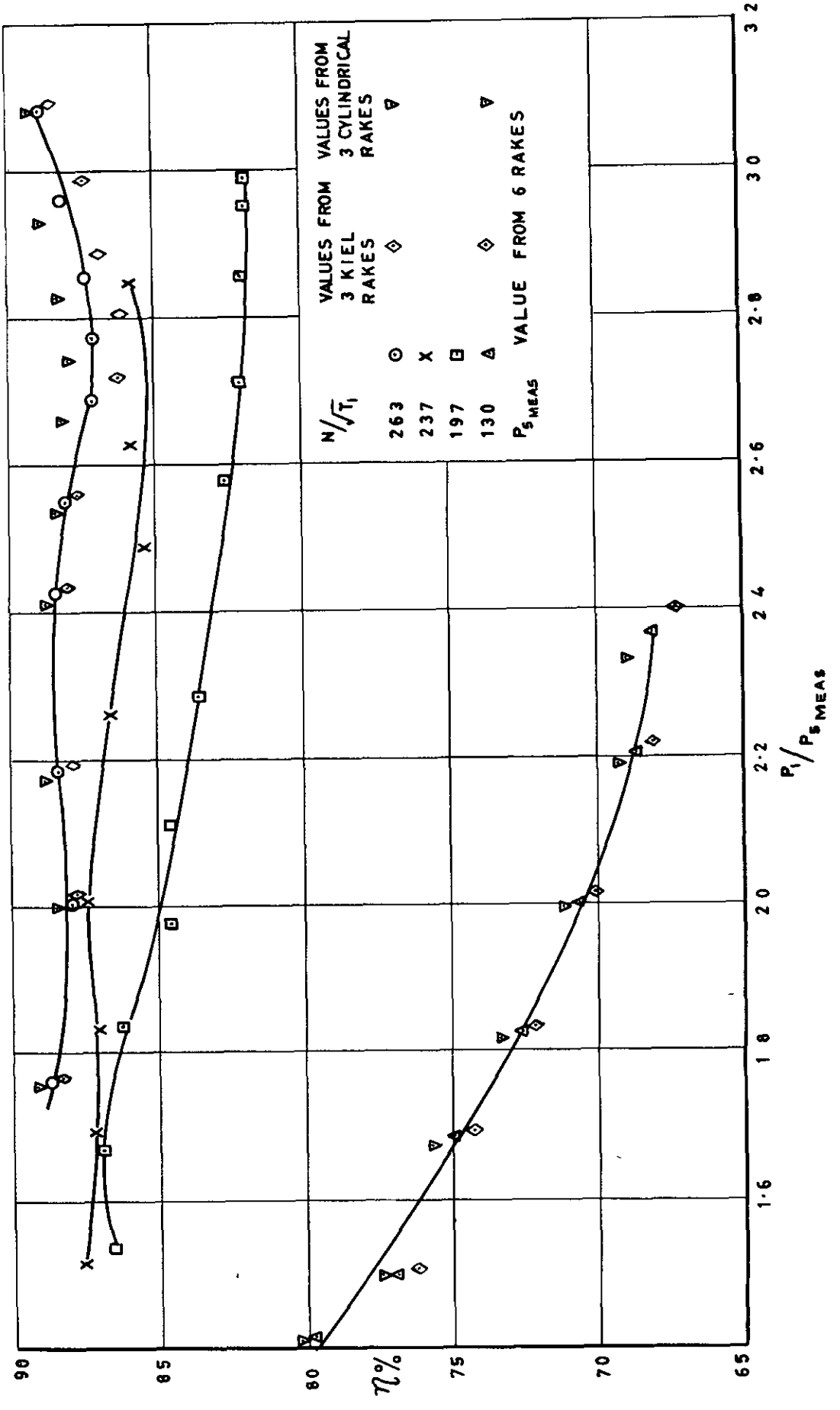

SERIES 1 (EFFICIENCY – $P_{S\ MEAS}$)

TWO STAGE – DATUM BLADES.

FIG. 11

$$\frac{P-\bar{p}_s}{\bar{P}_s-\bar{p}_s} = \frac{\text{LOCAL DYNAMIC HEAD}}{\text{MEAN DYNAMIC HEAD}}$$

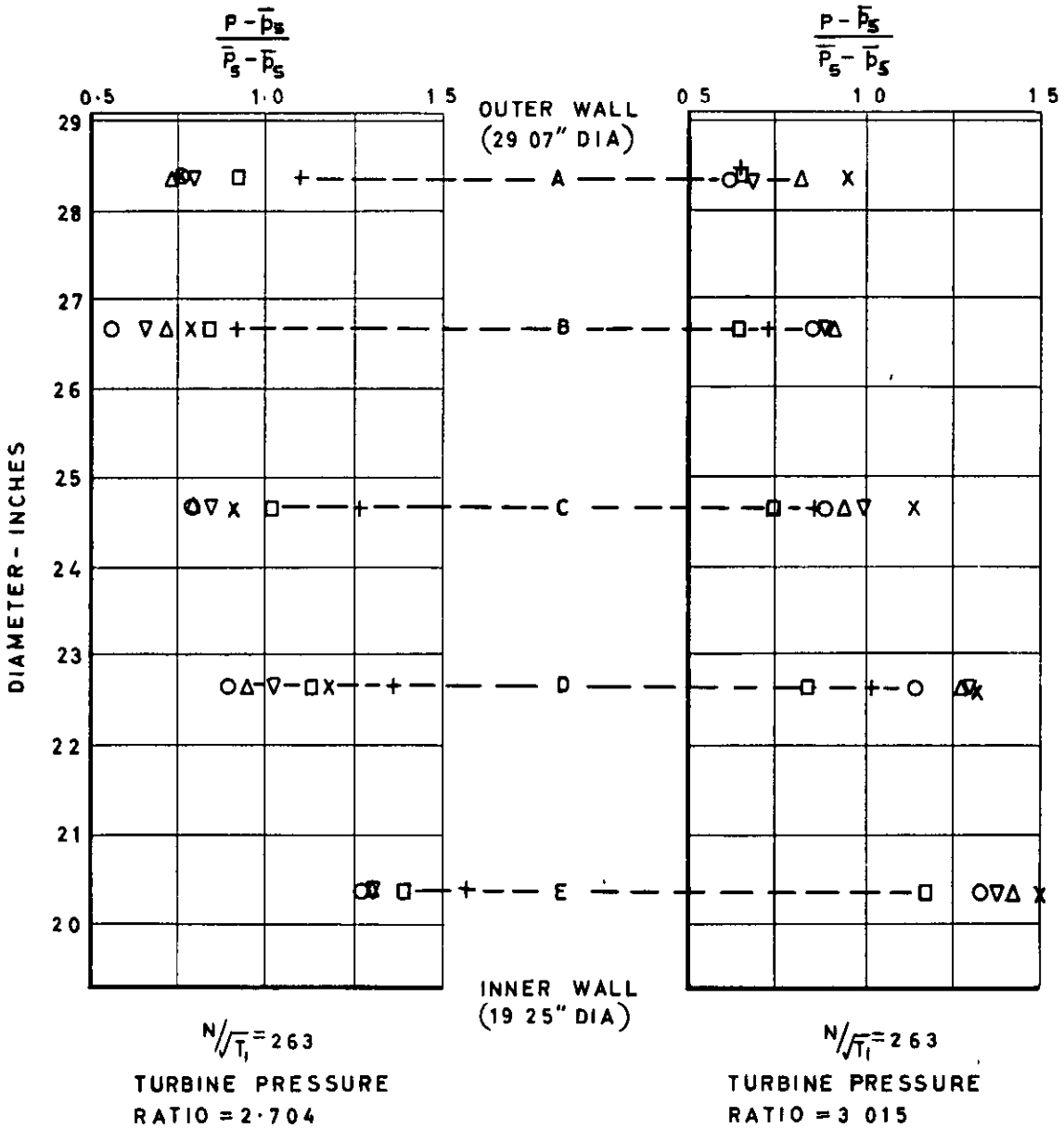

○ △ □ KIEL RAKES

▽ X + CYLINDRICAL PITOT RAKES

SERIES I (EXIT TOTAL PRESSURES - I)

TWO—STAGE DATUM BLADES.

FIG. 12

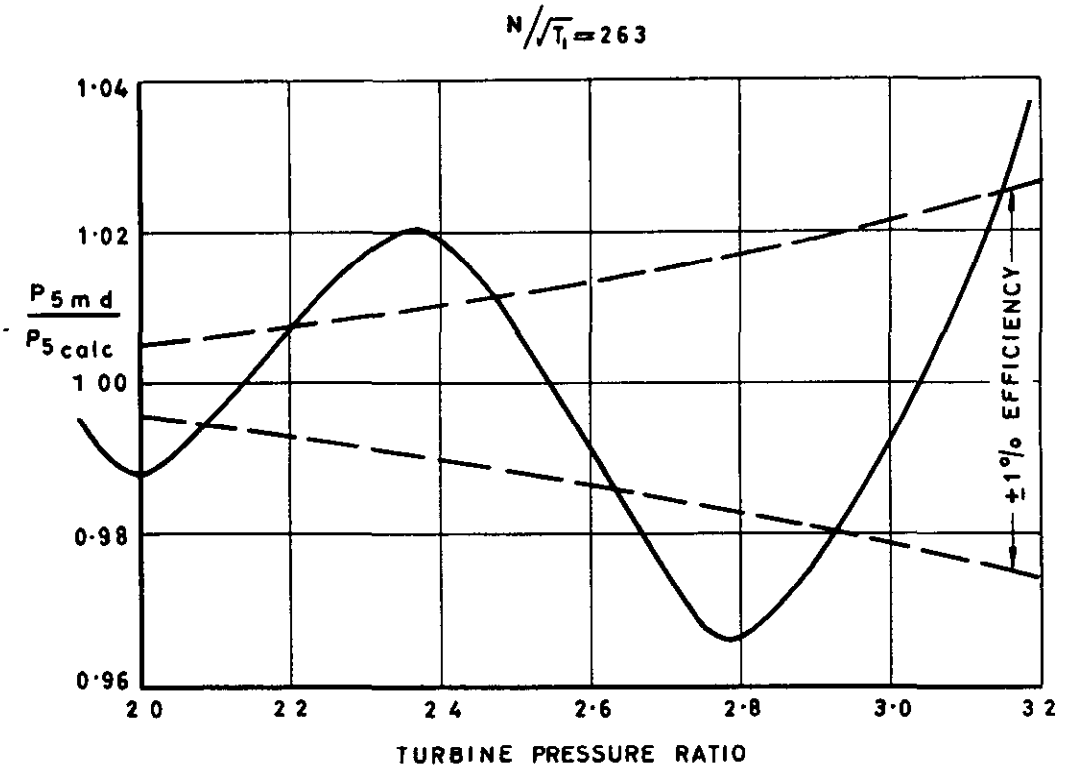

(a) LOCAL PRESSURE AT MEAN DIAMETER $P_{5\,m\,d}$. COMPARED WITH THE CONTINUITY VALUE $P_{5\,calc}$.

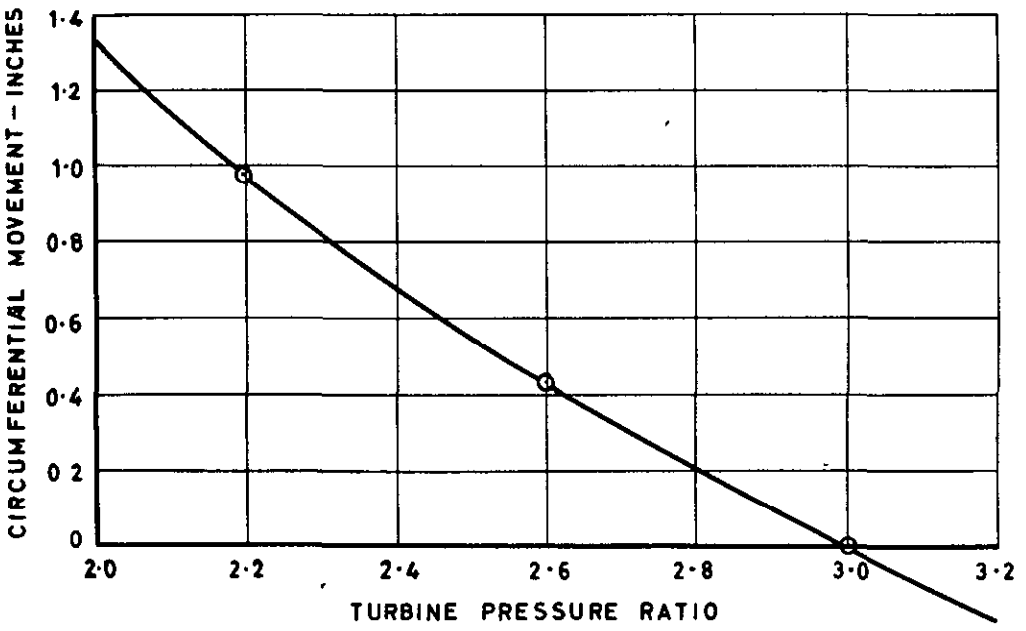

(b) CIRCUMFERENTIAL MOVEMENT OF STATOR WAKE.

SERIES 1 (EXIT TOTAL PRESSURES-2) TWO STAGE – DATUM BLADES.

FIG. 13

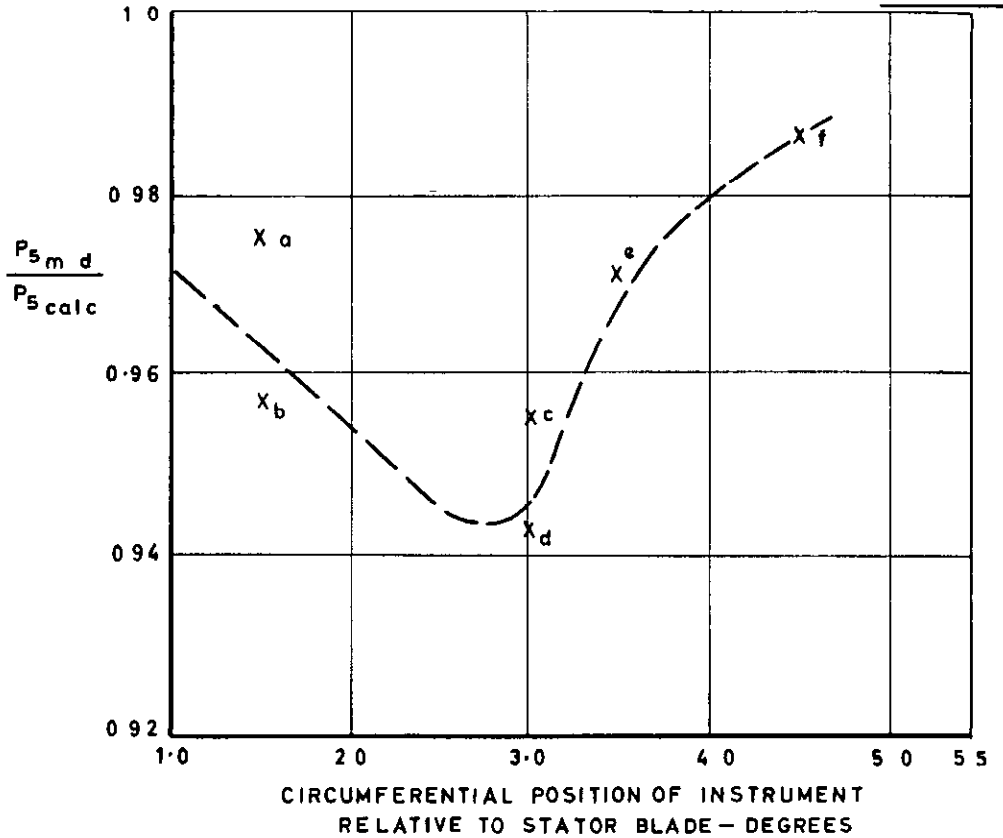

(a) MEAN DIAMETER TOTAL PRESSURES AT TURBINE EXIT IN RELATION TO STATOR BLADE PITCH.

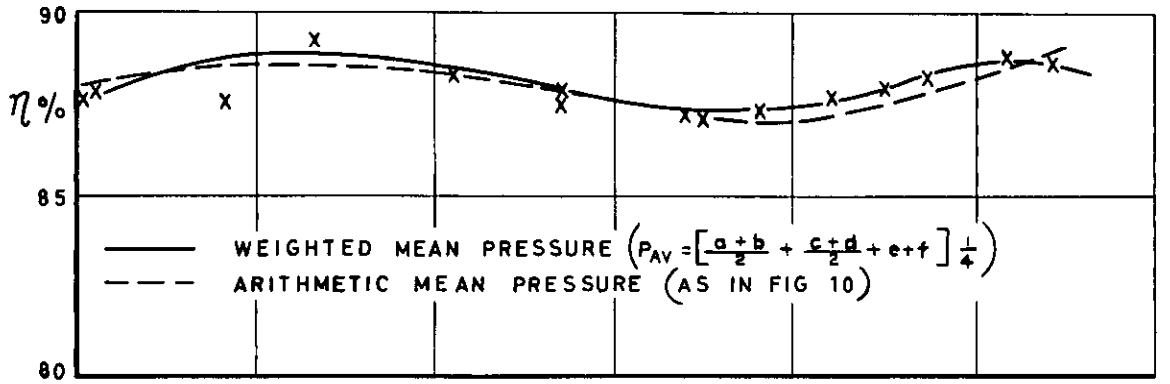

(b) THE EFFECT OF A WEIGHTED MEAN EXIT PRESSURE ON TURBINE EFFICIENCY.

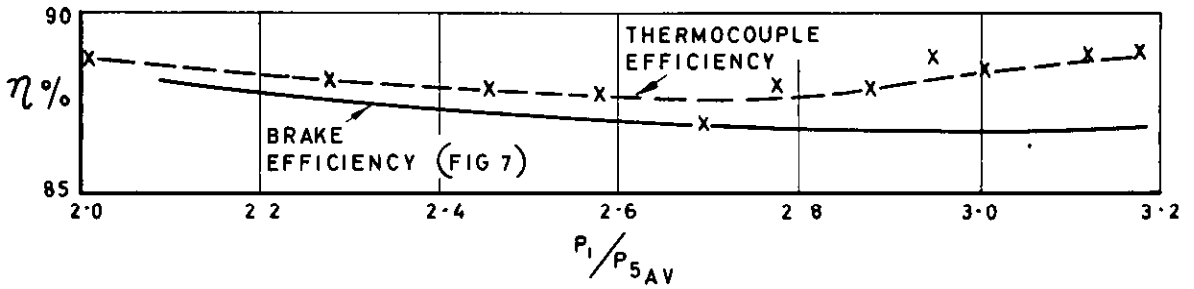

(c) COMPARISON BETWEEN 'BRAKE' & 'THERMOCOUPLE' EFFICIENCIES.

SERIES I (EXIT TOTAL PRESSURES-3)
TWO STAGE – DATUM BLADES.

FIG. 14

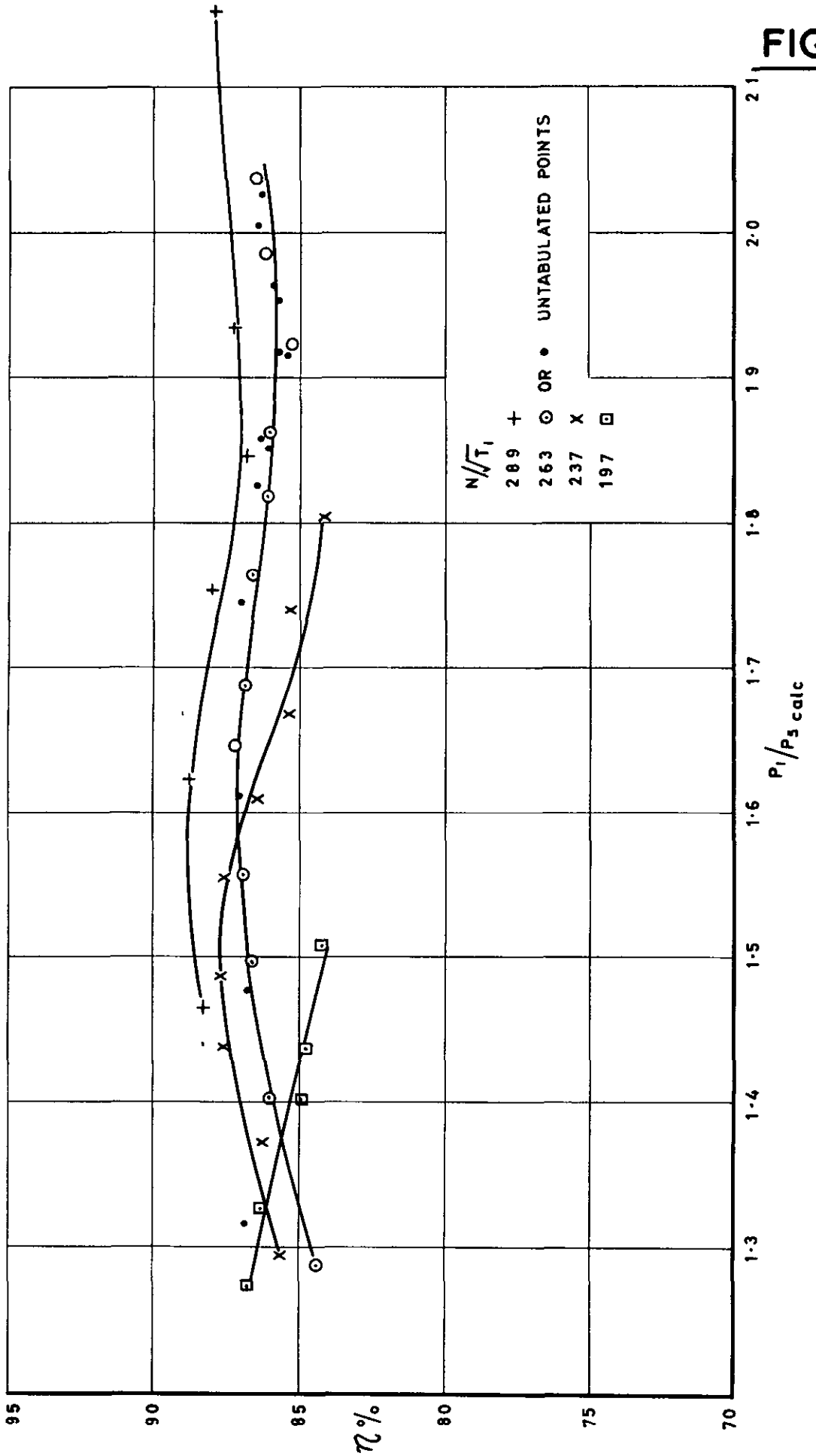

SERIES 2 (EFFICIENCY— $P_{5\ CALC.}$)
SINGLE STAGE—DATUM BLADES.

FIG. 15

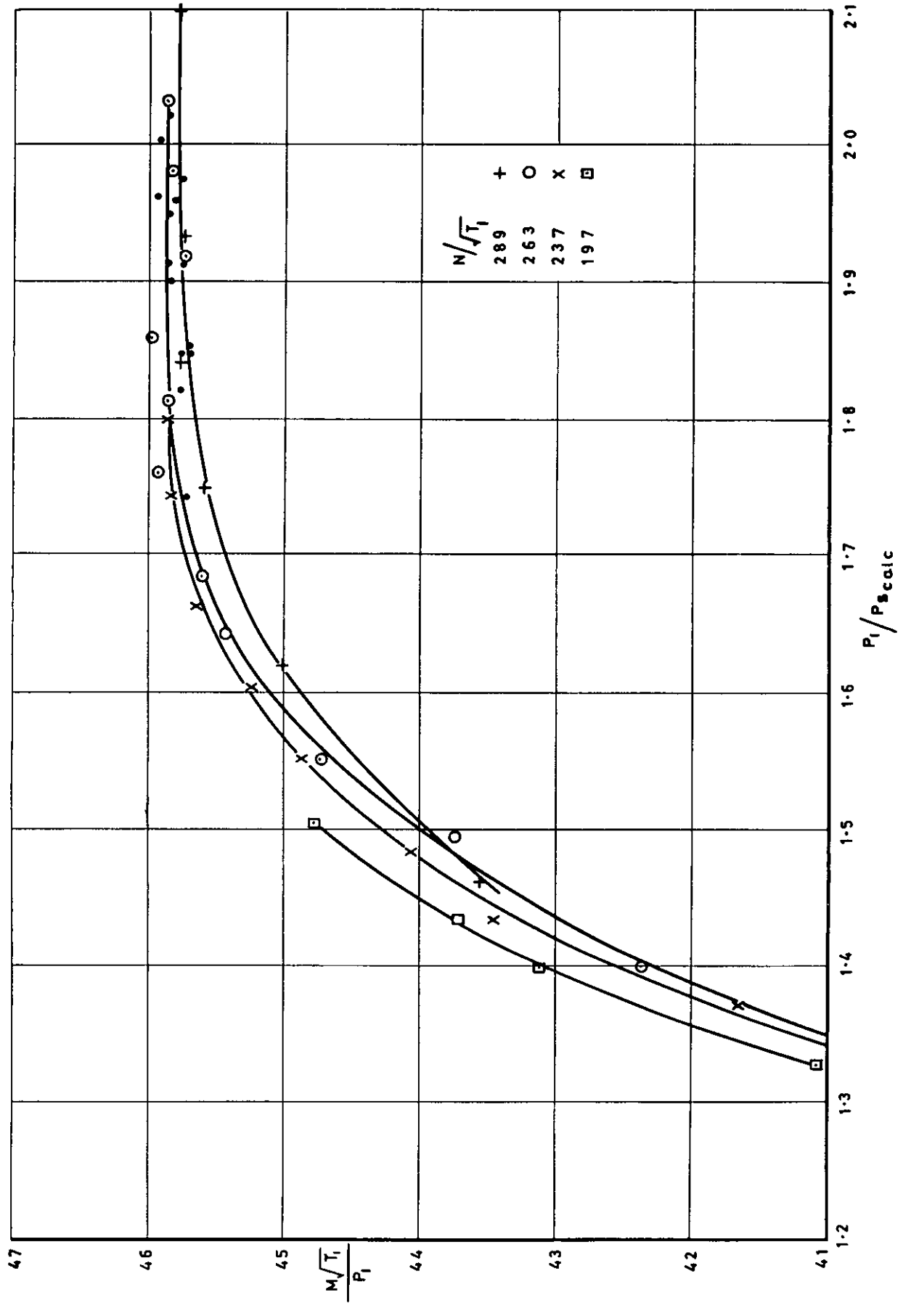

SERIES 2 (FLOW)
SINGLE STAGE – DATUM BLADES.

FIG. 16

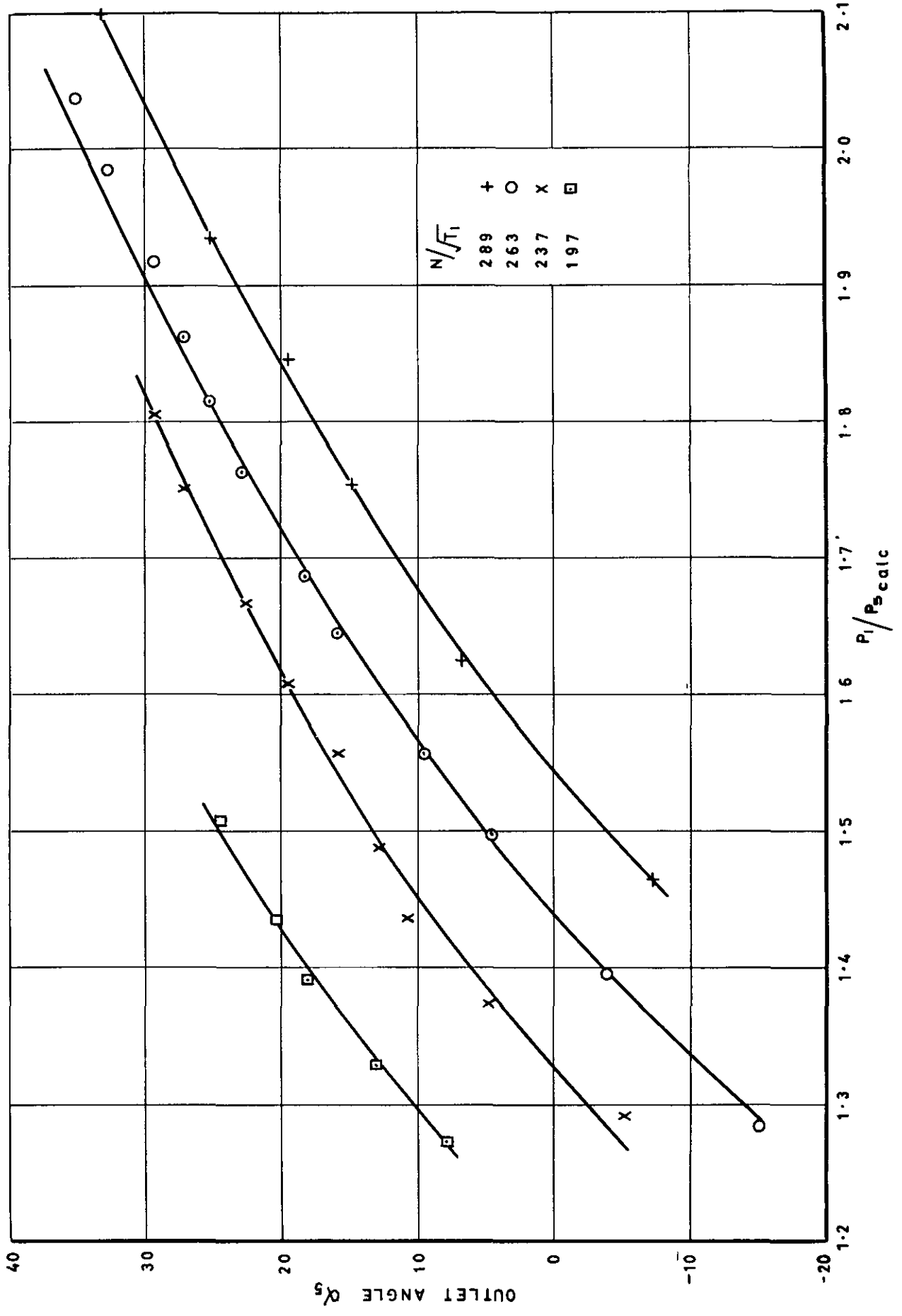

SERIES 2 (EXIT SWIRL)
SINGLE STAGE-DATUM BLADES.

FIG. 17

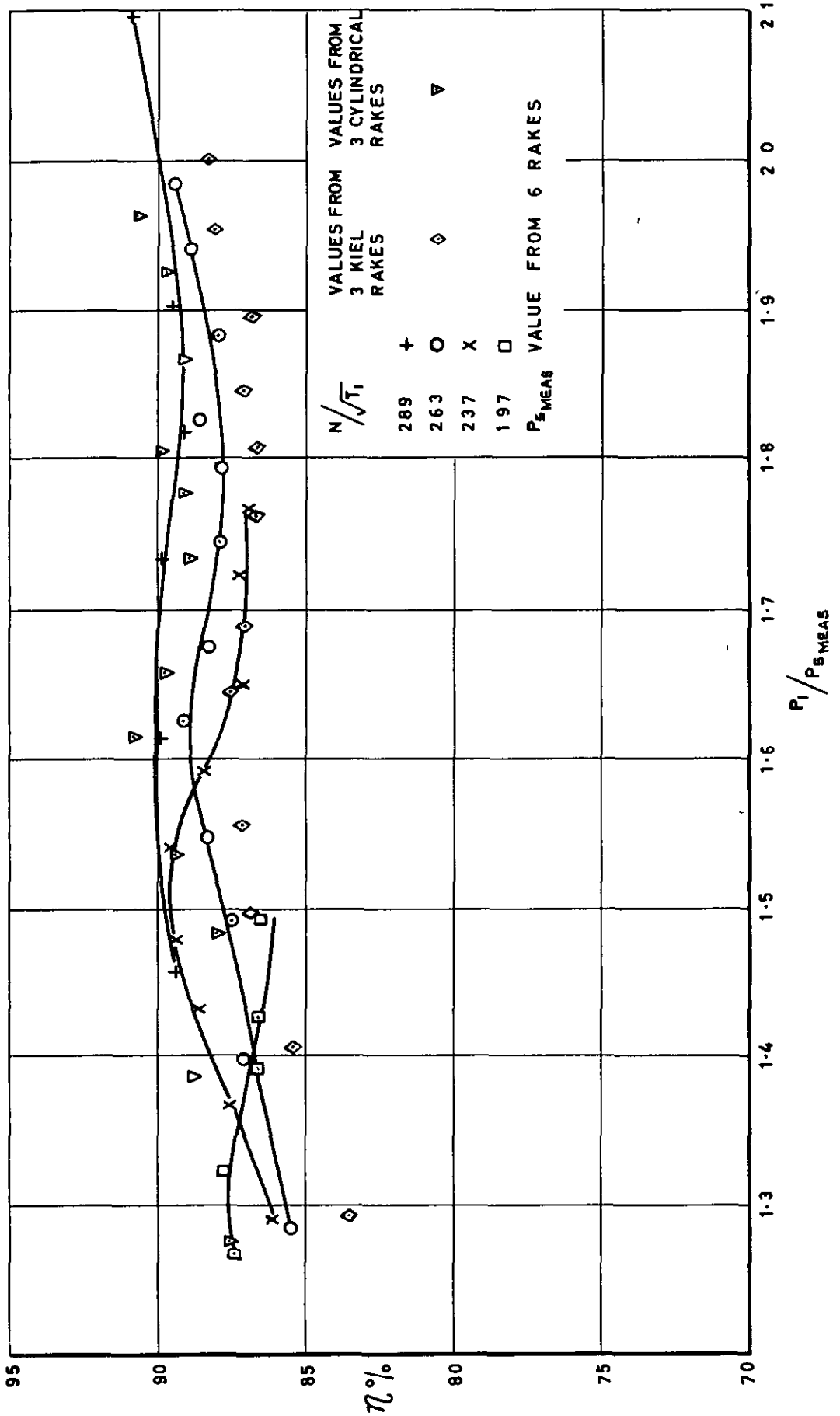

SERIES 2 (EFFICIENCY — $P_{5_{MEAS}}$)

SINGLE STAGE - DATUM BLADES.

FIG. 18

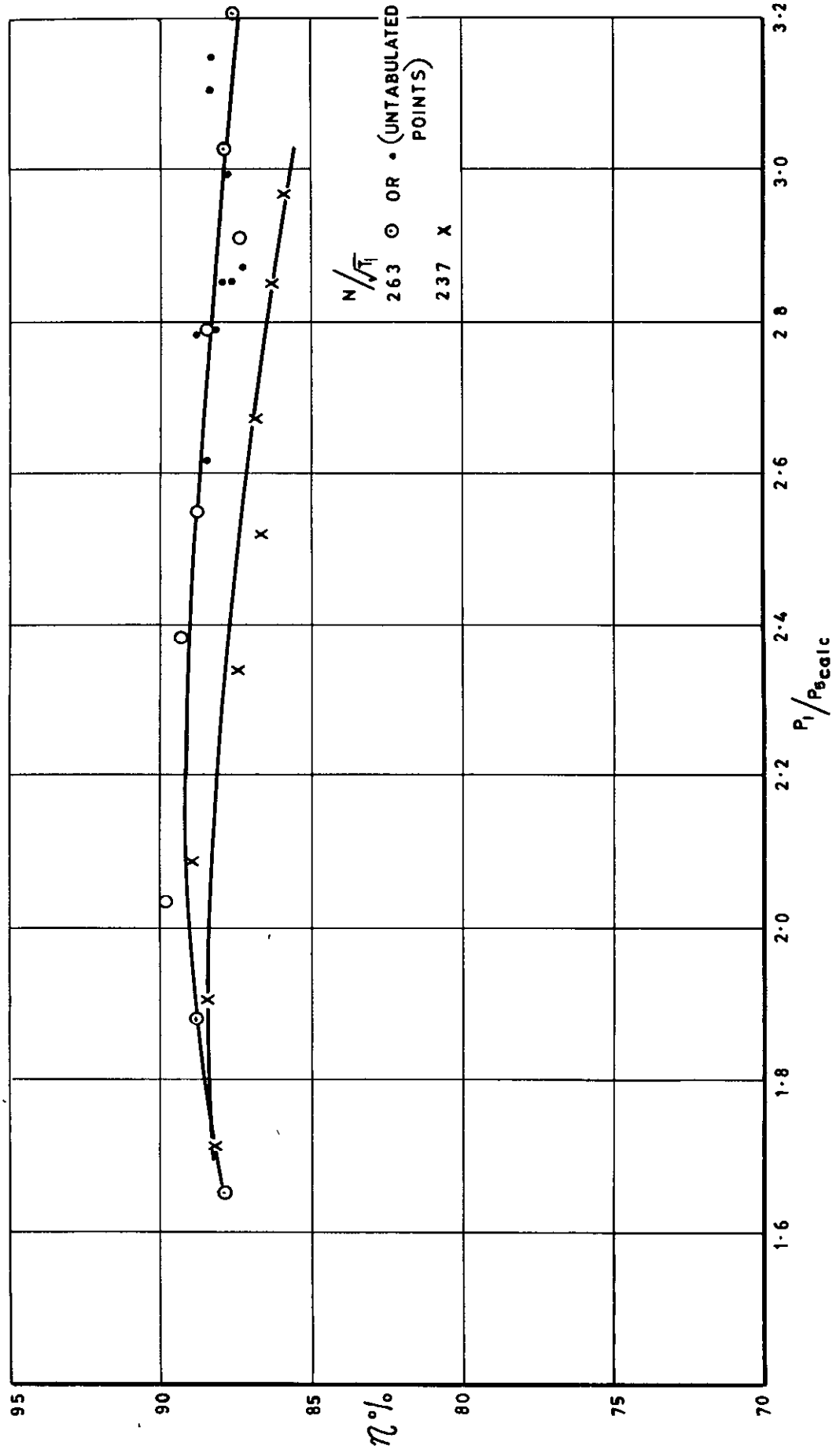

SERIES 3 (η – $P_{5_{CALC.}}$)

TWO STAGE – NEW BLADES.

FIG. 19

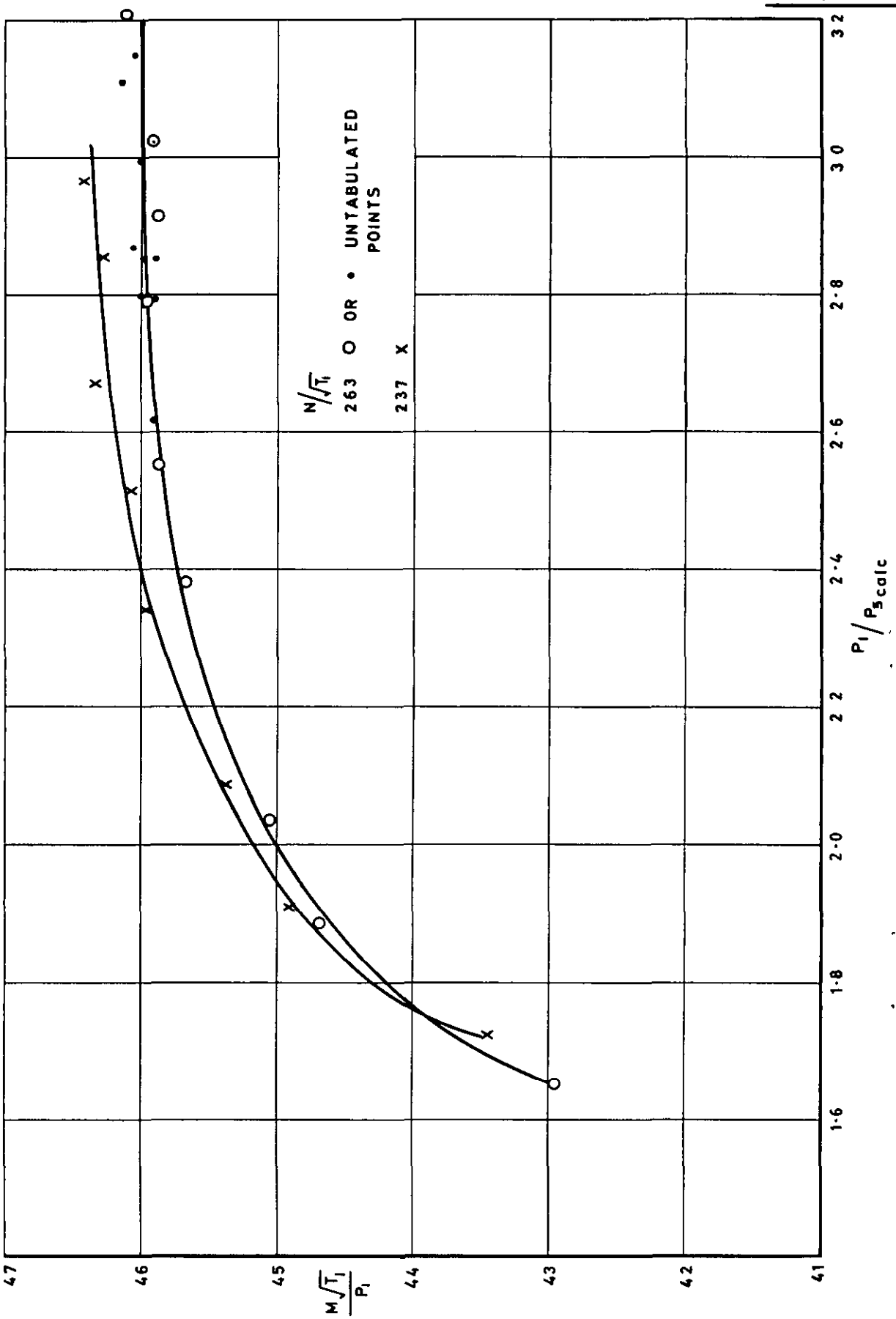

SERIES 3 (FLOW)

TWO STAGE-NEW BLADES.

FIG. 20

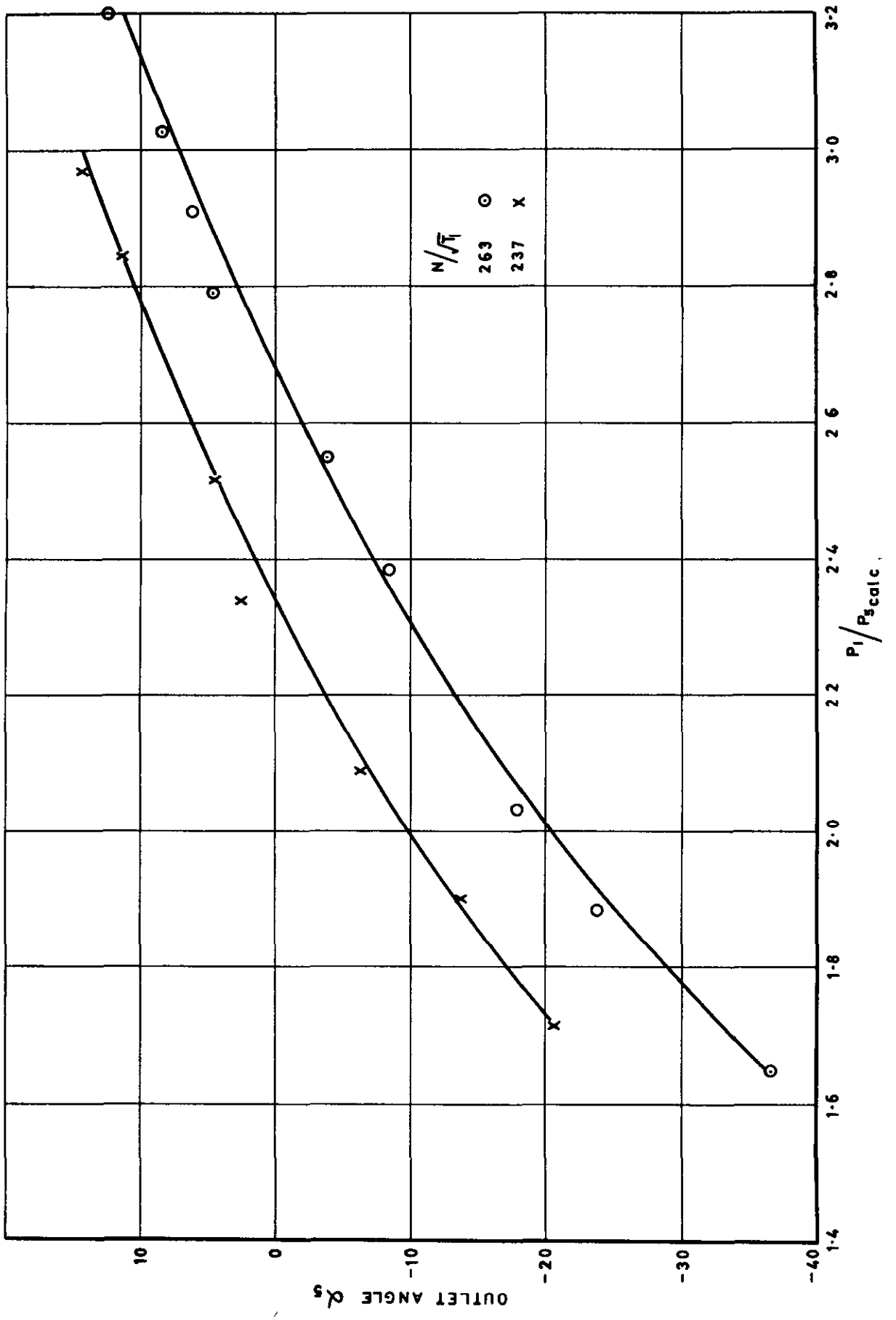

SERIES 3 (EXIT SWIRL)
TWO STAGE-NEW BLADES.

FIG. 21

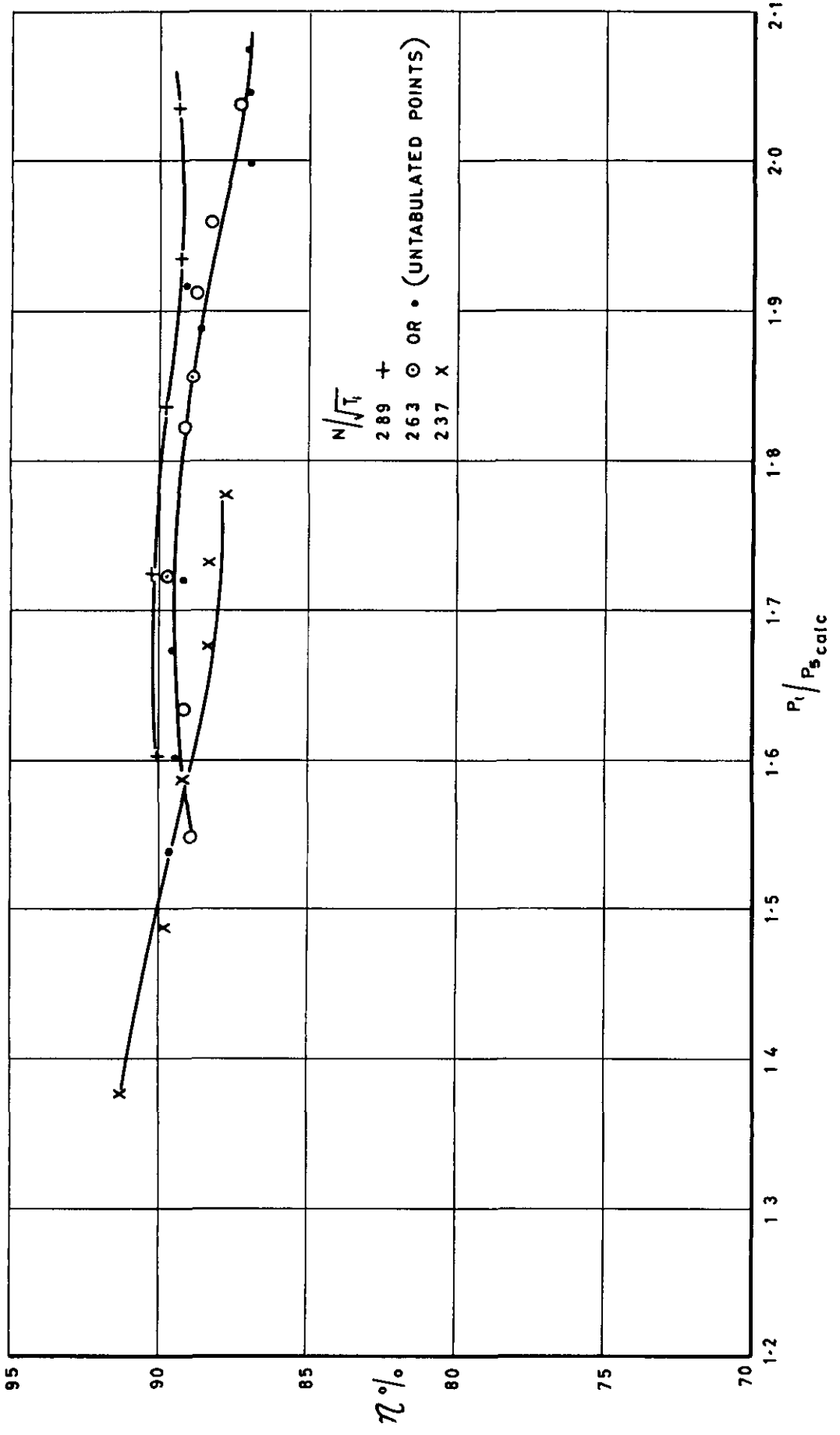

SERIES 4 (EFFICIENCY – $P_{5\,CALC.}$)

SINGLE STAGE – NEW BLADES.

SERIES 4 (FLOW)

SINGLE STAGE - NEW BLADES.

FIG. 22

FIG. 23

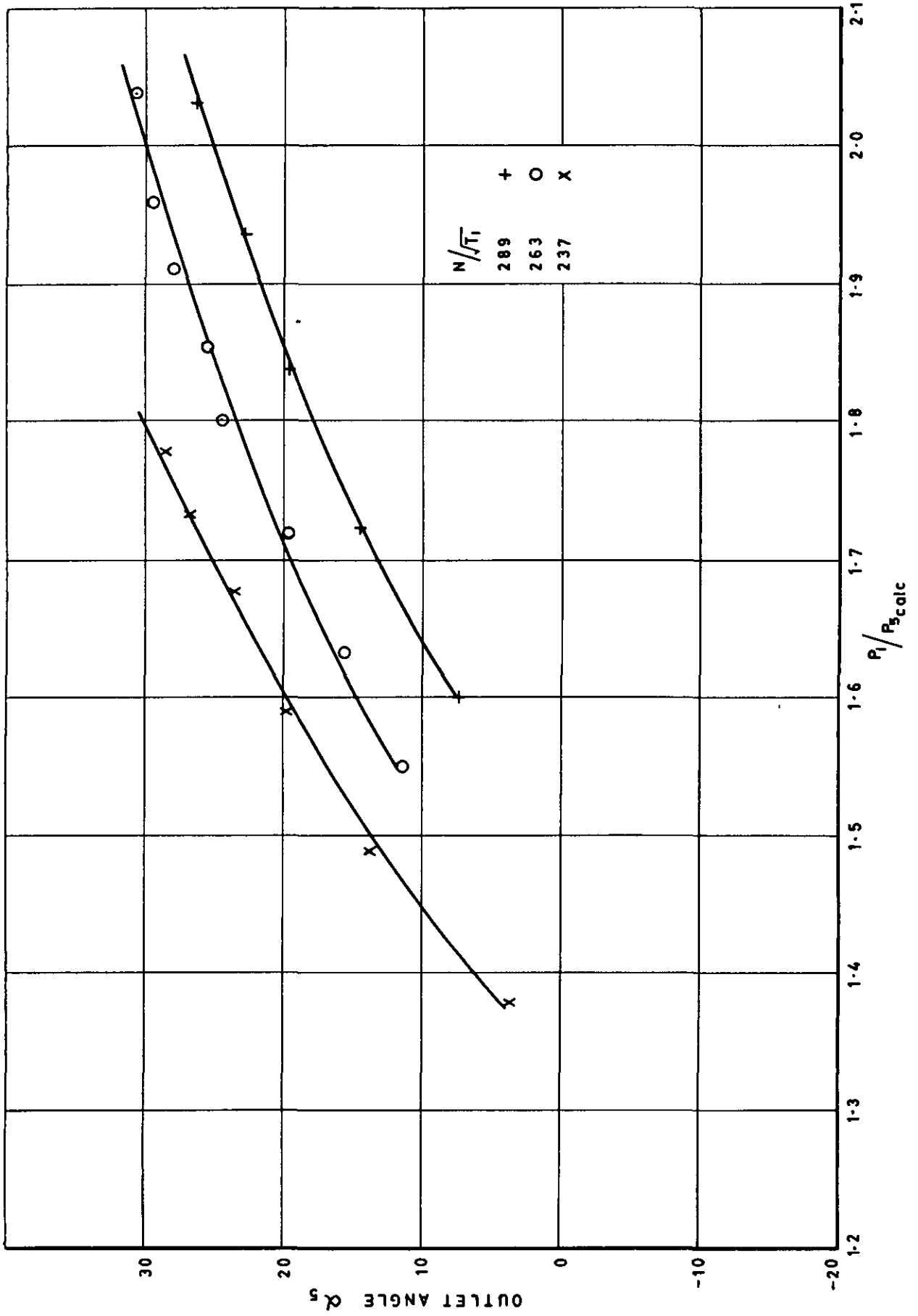

SERIES 4 (EXIT SWIRL)
SINGLE STAGE - NEW BLADES.

FIG. 24

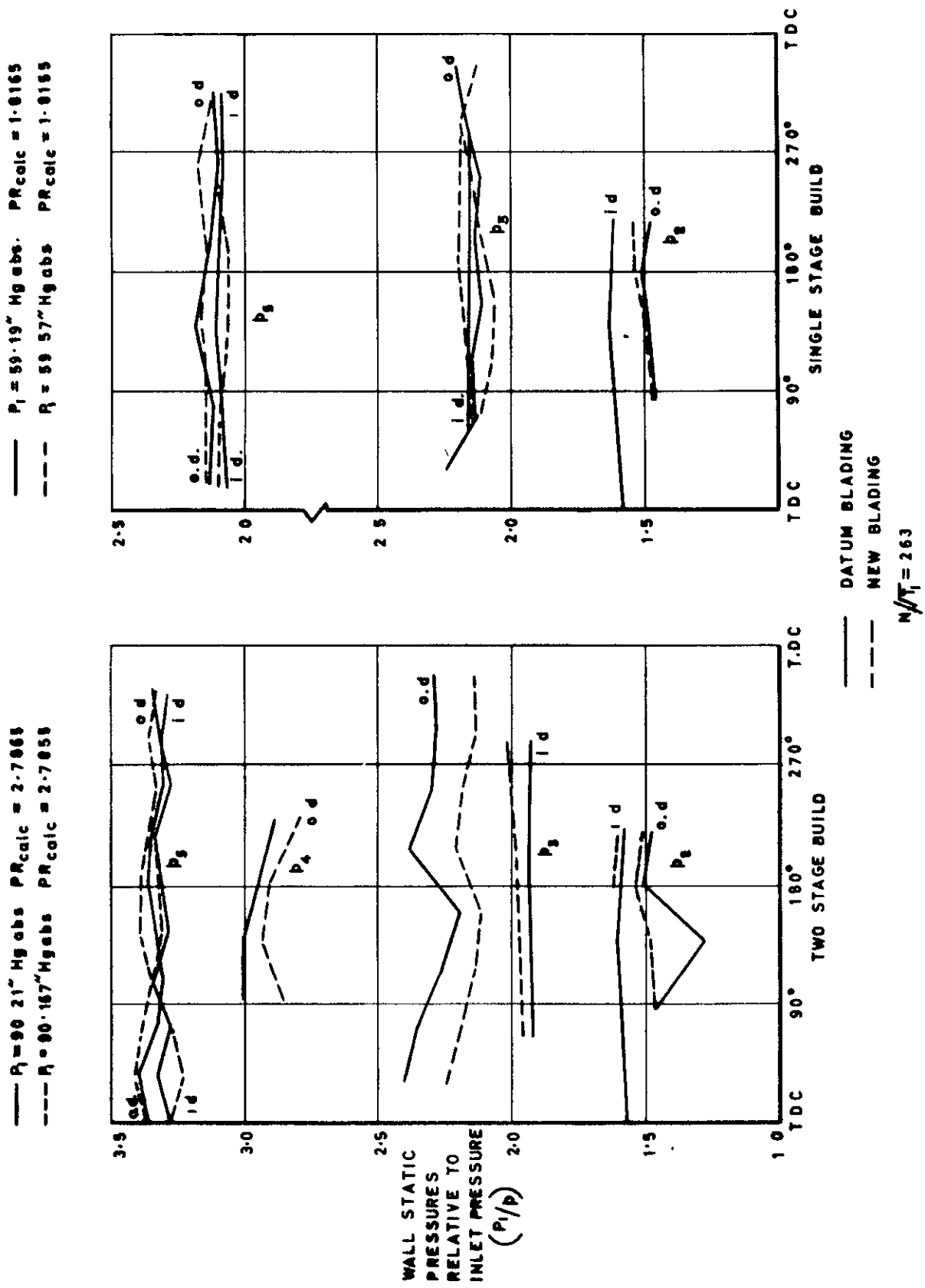

STATIC PRESSURE DISTRIBUTIONS IN THE TURBINE.

FIG. 25

TWO STAGE EFFICIENCIES

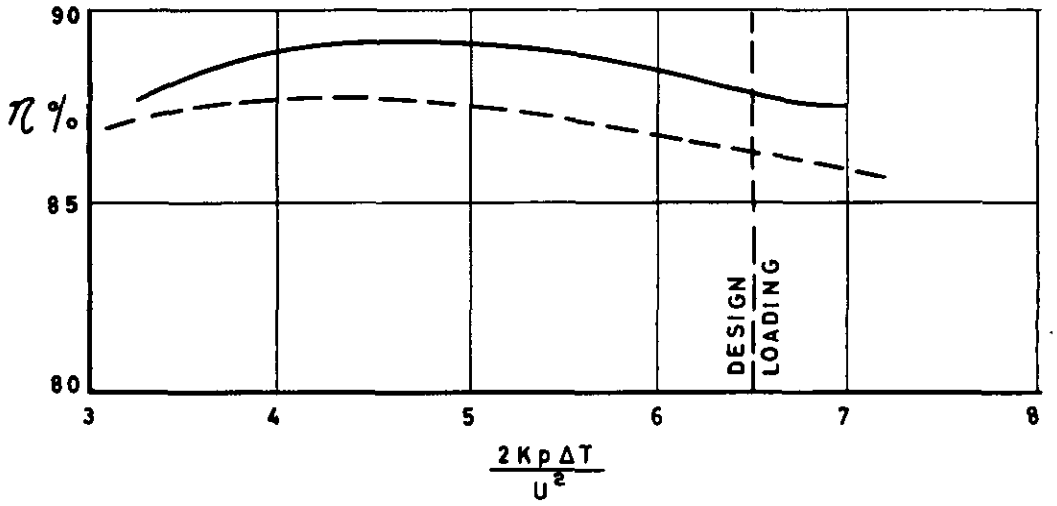

SINGLE STAGE EFFICIENCIES

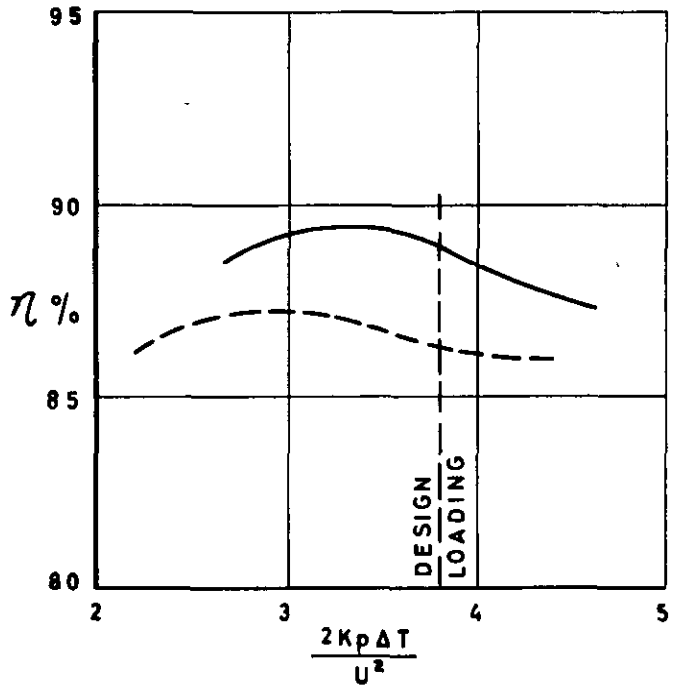

(CURVES BASED ON RESULTS FOR $N/\sqrt{T_1} = 263$ [DESIGN SPEED] & $N/\sqrt{T_1} = 237$)

COMPARISON OF STAGE EFFICIENCIES.

FIG. 26

SINGLE STAGE DATUM BLADES P R=1 84 $N/\sqrt{T_1}=263$

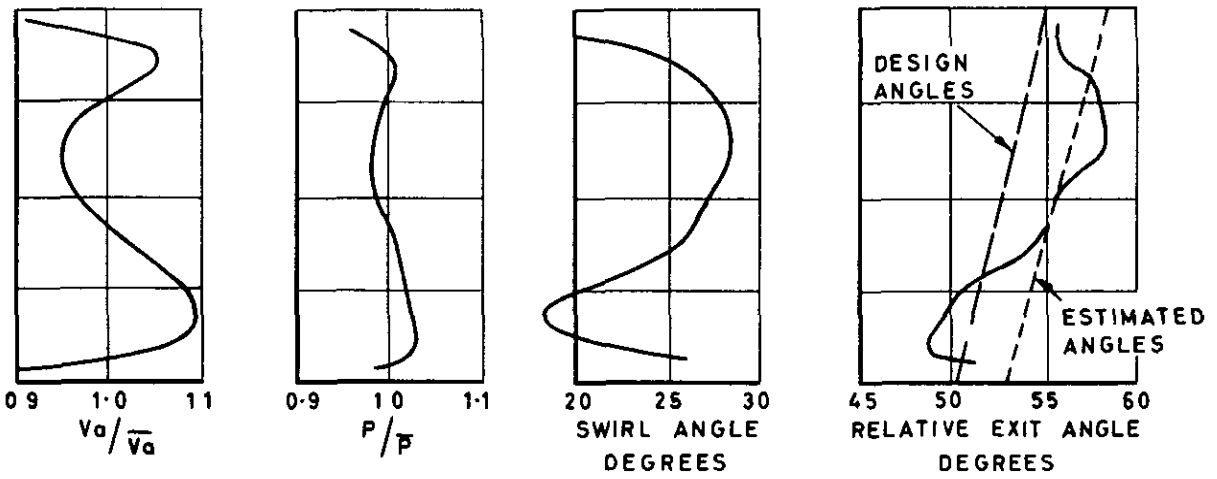

SINGLE STAGE NEW BLADES P R.=1·78 $N/\sqrt{T_1}=263$

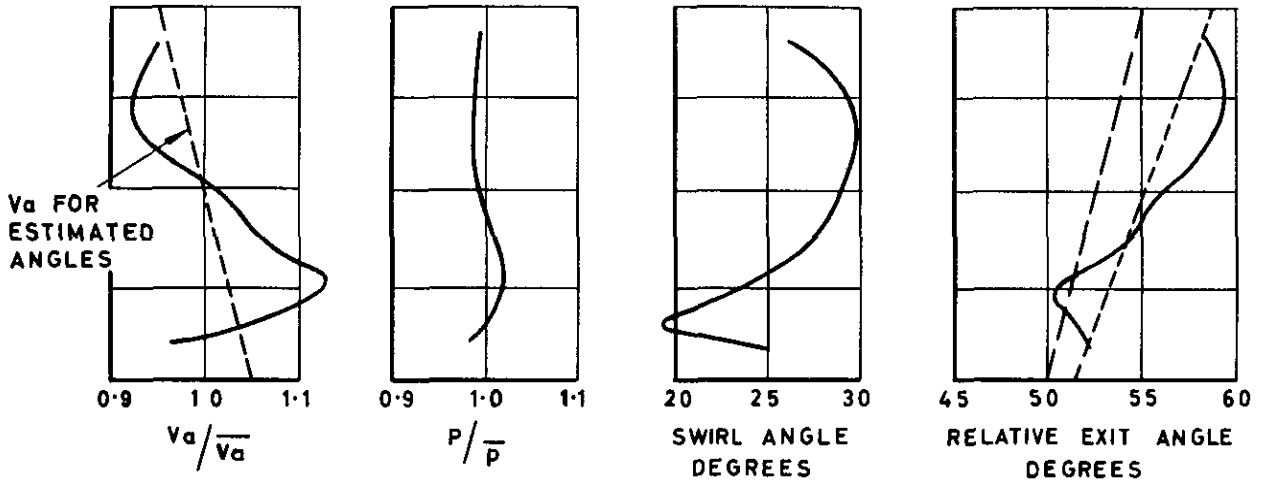

COMPARISON BETWEEN MEASURED AND CALCULATED MEAN RELATIVE OUTLET ANGLES.

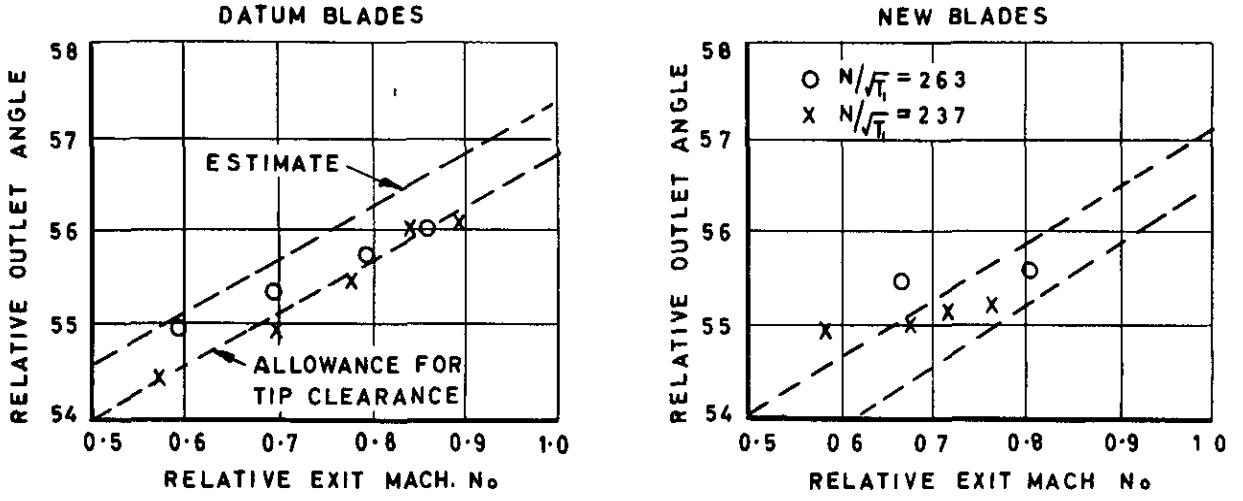

EXIT TRAVERSES FOR SERIES 2 & 4.

FIG. 2 7

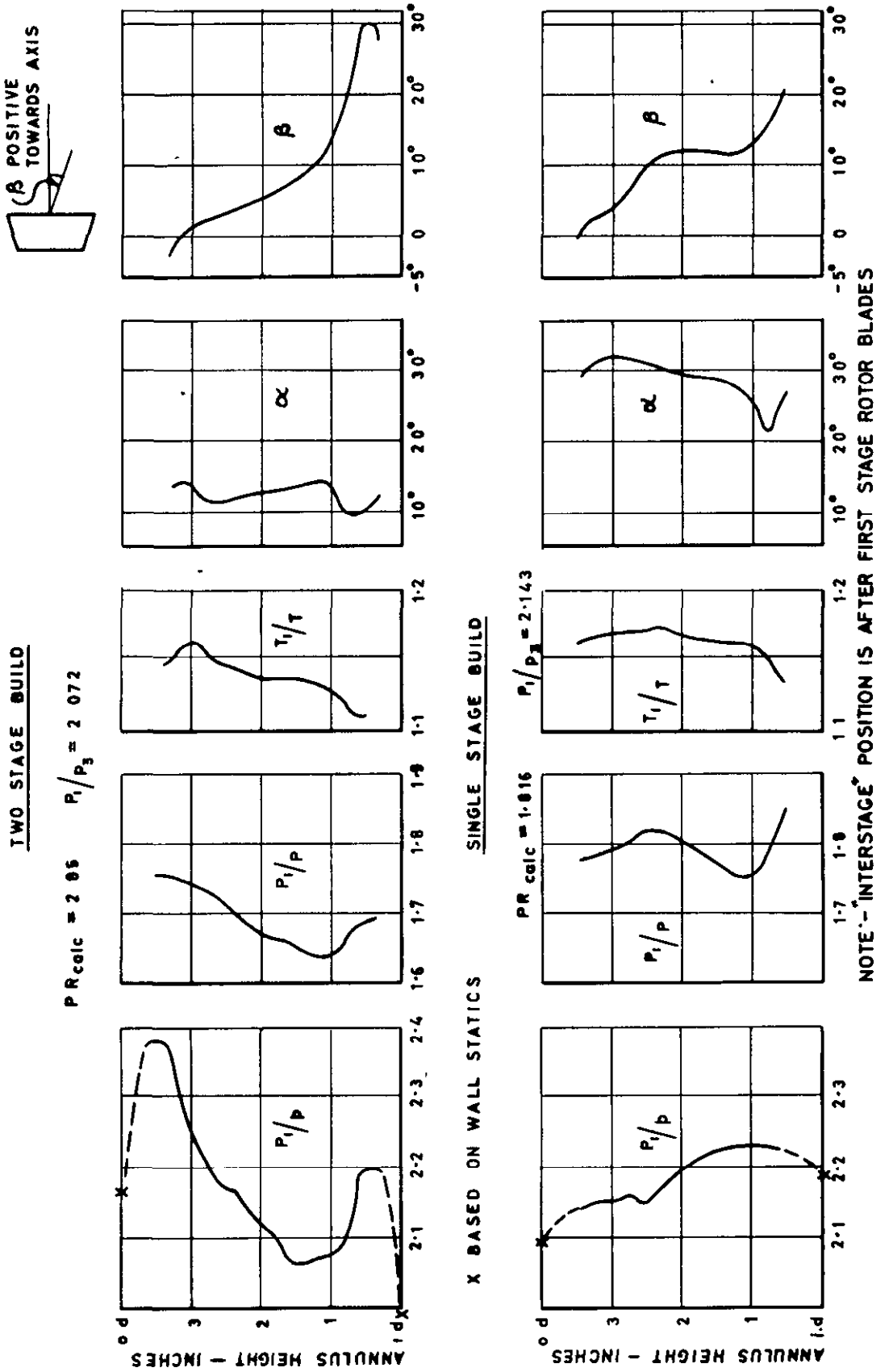

RESULTS OF "INTERSTAGE" TRAVERSES AT $N/\sqrt{T_1} = 263$ (A).

FIG. 28

AXIAL VELOCITY PROFILE
AT ROTOR BLADE EXIT.
(FIRST STAGE)

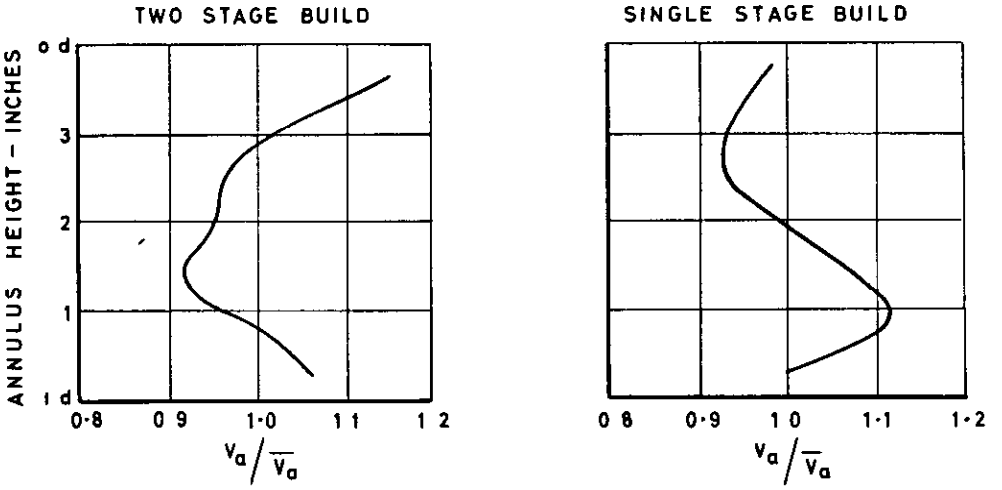

RADIAL DISTRIBUTION
OF TEMPERATURE DROP IN FIRST STAGE

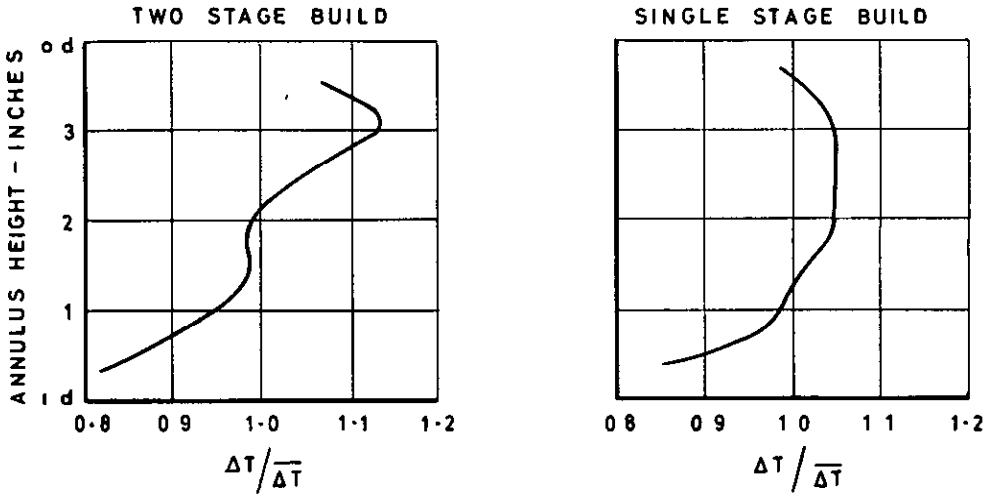

RESULTS OF "INTERSTAGE" TRAVERSES AT $N/\sqrt{T_1} = 263$ (B).

FIG. 29

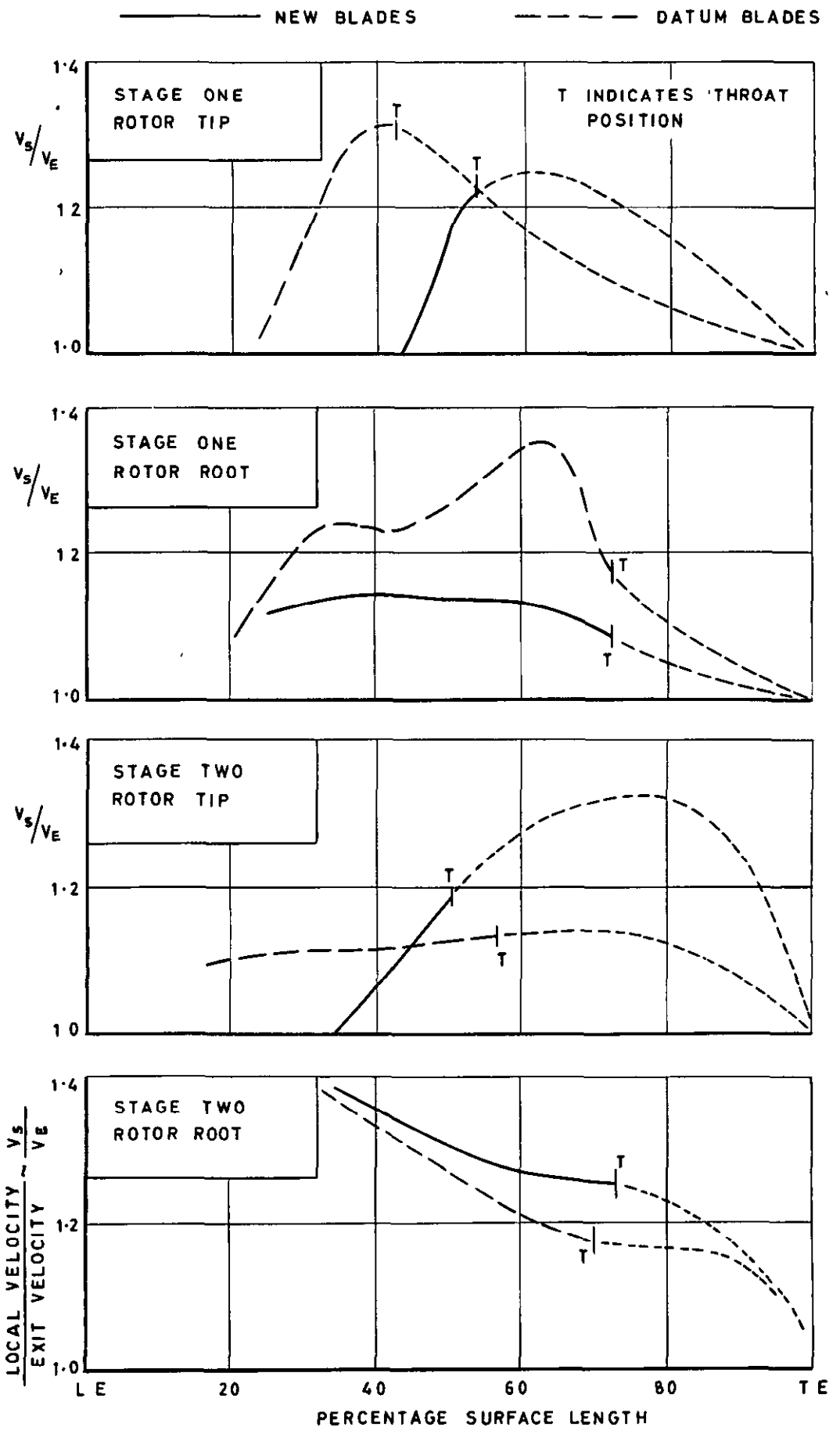

VELOCITY DISTRIBUTIONS ON BLADE SUCTION SURFACES.

A.R.C. C.P. No. 941 621.438-253.5:621.001.1
October, 1965
Johnston, I. H. and Smart, D. E.

AN EXPERIMENT IN TURBINE BLADE PROFILE DESIGN

Part I of this Report describes a method for designing the blades of highly loaded two-stage turbine on the basis of certain design parameters derived from an efficient turbine of lower loading. Part II presents the test performances measured with the original and new blades when tested in both single-stage and two-stage configurations. A full and detailed presentation of the experimental work is given to illustrate the problems in instrumentation and in interpretation of test measurements which were encountered.

The new blades give an improvement in the efficiency of the first stage, but the performance of the second stage remains unchanged and an analysis of blade section velocity distributions gives additional proof of the shortcomings of an essentially empirical design approach.

A.R.C. C.P. No. 941 621.438-253.5:621.001.1
October, 1965
Johnston, I. H. and Smart, D. E.

AN EXPERIMENT IN TURBINE BLADE PROFILE DESIGN

Part I of this Report describes a method for designing the blades of highly loaded two-stage turbine on the basis of certain design parameters derived from an efficient turbine of lower loading. Part II presents the test performances measured with the original and new blades when tested in both single-stage and two-stage configurations. A full and detailed presentation of the experimental work is given to illustrate the problems in instrumentation and in interpretation of test measurements which were encountered.

The new blades give an improvement in the efficiency of the first stage, but the performance of the second stage remains unchanged and an analysis of blade section velocity distributions gives additional proof of the shortcomings of an essentially empirical design approach.

A.R.C. C.P. No. 941 621.438-253.5:621.001.1
October, 1965
Johnston, I. H. and Smart, D. E.

AN EXPERIMENT IN TURBINE BLADE PROFILE DESIGN

Part I of this Report describes a method for designing the blades of highly loaded two-stage turbine on the basis of certain design parameters derived from an efficient turbine of lower loading. Part II presents the test performances measured with the original and new blades when tested in both single-stage and two-stage configurations. A full and detailed presentation of the experimental work is given to illustrate the problems in instrumentation and in interpretation of test measurements which were encountered.

The new blades give an improvement in the efficiency of the first stage, but the performance of the second stage remains unchanged and an analysis of blade section velocity distributions gives additional proof of the shortcomings of an essentially empirical design approach.

DETACHABLE ABSTRACT CARDS

Printed and published by
HER MAJESTY'S STATIONERY OFFICE

To be purchased from
49 High Holborn, London W C 1
423 Oxford Street, London W.1
13A Castle Street, Edinburgh 2
109 St Mary Street, Cardiff
Brazennose Street, Manchester 2
50 Fairfax Street, Bristol 1
35 Smallbrook, Ringway, Birmingham 5
7 - 11 Linenhall Street, Belfast 2
or through any bookseller

Printed in England

C.P. No. 941

S O Code No 23-9017-41